Experimental Parasitology 142 (2014) 67–82

Contents lists available at ScienceDirect

Experimental Parasitology

journal homepage: www.elsevier.com/locate/yexpr

Tritrichomonas foetus: Characterisation of ecto-phosphatase activities in the endoflagelar form and their possible participation on the parasite's transformation and cytotoxicity

Antonio Pereira-Neves [a,b,c], José Luis Rosales-Encina [d], José Roberto Meyer-Fernandes [c,e], Marlene Benchimol [b,c,*]

[a] Programa de Pós-graduação em Ciências Morfológicas da Universidade Federal do Rio de Janeiro CCS, bloco F, Cidade Universitária, Ilha do Fundão, CEP 21941-521 Rio de Janeiro, RJ, Brazil
[b] Laboratório de Ultraestrutura Celular, Universidade Santa Úrsula, Rua Jornalista Orlando Dantas 59, Botafogo, CEP 22231-010 Rio de Janeiro, Brazil
[c] Instituto Nacional de Ciência e Tecnologia de Biologia Estrutural e Bioimagem, Cidade Universitária, Ilha do Fundão, CEP 21941-521 Rio de Janeiro, RJ, Brazil
[d] Departamento de Infectómica y Patogénesis Molecular, Centro de Investigación y de Estudios Avanzados del I.P.N., México D.F. 07360, Mexico
[e] Laboratório de Bioquímica Celular, Instituto de Bioquímica Médica, Centro de Ciências da Saúde, Universidade Federal do Rio de Janeiro, bloco H, Cidade Universitária, Ilha do Fundão, CEP 21941-521 Rio de Janeiro, RJ, Brazil

HIGHLIGHTS

- Distinct ecto-phosphatase activities were detected between both *T. foetus*-forms.
- A correlation between ecto-phosphatase and pseudocyst formation was observed.
- A relationship was observed between ecto-phosphatase and cytotoxicity of *T. foetus*.
- Ecto-phosphatase activity could be involved in the pseudocyst transformation.
- Ecto-phosphatase activity could represent a virulence factor for *T. foetus*.

GRAPHICAL ABSTRACT

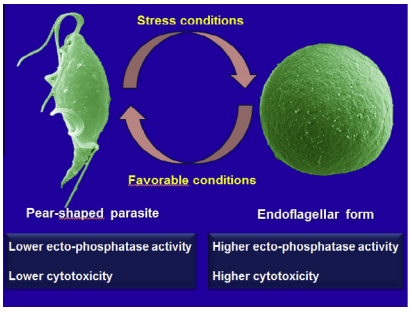

ARTICLE INFO

Article history:
Received 5 February 2014
Received in revised form 12 April 2014
Accepted 14 April 2014
Available online 30 April 2014

Keywords:
Cytotoxicity
Ecto-enzymes
Ecto-phosphatase
Pseudocyst
Protein tyrosine phosphatase

ABSTRACT

The protist parasite *Tritrichomonas foetus* displays a pear-shaped (PS) and a pseudocystic or endoflagellar form (EFF). Here, we characterised the ecto-phosphatase activity on the surface of EFF and compare its biochemical properties to that of the PS regarding rate of substrate hydrolysis, pH activation profile and sensitivity to well-known phosphatases inhibitors. Two strains exhibiting low- and high-cytotoxicity were used. The enzyme activities of PS and EFF exhibited similar characteristics of protein tyrosine phosphatases (PTP). However, the ecto-phosphatase activities for both forms presented distinct kinetic parameters and different inhibition patterns by PTP inhibitors, suggesting the presence of distinct ecto-enzyme activities between PS and EFF, as well, between both strains. Ultrastructural cytochemistry confirmed the differential distribution of the ecto-phosphatase activity during the EFF transformation. An increase in the percentage of the EFF resulted in a proportional increase in the ecto-phosphatase activity. During EFF reversion, ecto-phosphatase activity decreased and was restored to the level found in the parasites before EFF induction. PS and EFF from the high-cytotoxic strain exhibited higher ecto-phosphatase activities than PS and EFF from the low-cytotoxic strain, respectively. In both strains, the EFF was more

* Corresponding author at: Laboratório de Ultraestrutura Celular, Universidade Santa Úrsula, Rua Jornalista Orlando Dantas 59, Botafogo, 22231-010 Rio de Janeiro, Brazil. Fax: +55 21 22370440.
E-mail address: marlenebenchimol@gmail.com (M. Benchimol).

http://dx.doi.org/10.1016/j.exppara.2014.04.007

cytotoxic and exhibited higher ecto-phosphatase activity when compared to the PS. A large part of the ecto-phosphatase activities of EFF from both strains and PS from the high-cytotoxic strain was irreversibly inhibited when the parasites were pre-treated with a specific antibody against amoebic PTP (anti-EhPRL). Immunoreaction assays revealed that the anti-EhPRL antibody cross-reacted with a 24-kDa protein differentially expressed on the cell surface of PS and EFF *T. foetus*. A positive correlation was observed between the surface expression of 24-kDa protein and ecto-phosphatase activity. Irreversible inhibition of a part of the ecto-phosphatase activities partially blocked the EFF induction and the cytotoxic effects exerted by both forms. These results suggest that the ecto-phosphatase activities could play a role on the EFF transformation and cytotoxicity of *T. foetus*.

1. Introduction

Tritrichomonas foetus (Excavata: Parabasalia) is the causative agent of bovine trichomonosis, a devastating venereal disease that leads to reproductive failure in infected herds (Mardones et al., 2008). Bovine trichomonosis creates a serious economic burden in the South America, United States, Asia, Australia and in other areas of the world where open range management and natural breeding are practiced (BonDurant, 2005). Recently, *T. foetus* has also been recognised as the agent of feline trichomonosis, which is a large-bowel disease in domestic cats (Manning, 2010).

T. foetus has a simple life cycle consisting only of a trophozoitic form, which is characterised by a pear-shaped (PS) body, three anterior flagella and one recurrent flagellum. Under unfavourable environmental conditions, such as abrupt changes in temperature (Pereira-Neves et al., 2012) or in the presence of drugs, e.g. colchicine (Madeiro da Costa and Benchimol, 2004), the trophozoite undergoes profound morphological alterations and takes on an endoflagellar form (EFF), also known as pseudocyst. In this form, the parasite adopts a spherical or ellipsoid shape and internalises its flagella, but no cyst wall surrounds the cell. The EFF is a reversible and cytotoxic form that exhibits a distinct mitotic behaviour when compared to PS (Pereira-Neves et al., 2012). In addition, in preputial secretions from *T. foetus*-infected bulls, the EFF occurs more frequently than the PS (Pereira-Neves et al., 2011). Thus, studies to elucidate the role of EFF in the life cycle of *T. foetus* and their relationship with trichomonosis are gaining more importance.

Similar to the related human pathogen *Trichomonas vaginalis*, *T. foetus* is recognised as one of the most common sexually transmitted infectious agents. However, several aspects of its pathogenesis have to be fully defined. Therefore, the studies concerning the mechanisms and factors involved in the parasite's virulence are very important. In this context, the reversible protein tyrosine phosphorylation represents one of the key regulatory events that are critical to the control of many cellular, physiological and pathogenic processes (Heneberg, 2012). The control of protein tyrosine phosphorylation is regulated by the coupled action of two antagonistic classes of enzymes: protein tyrosine kinases and protein tyrosine phosphatases (PTPs).

PTPs comprise a large superfamily of enzymes that catalyse the removal of a phosphate group attached to a tyrosine residue, using a cysteinyl-phosphate enzyme intermediate. The cysteine-based PTPs share a common highly conserved signature motif, HC-(X_5)-R, in their active catalytic sites and can be divided into four evolutionary unrelated groups according to their sequence homology and substrate specificity: (a) classical PTPs; (b) dual specificity PTPs; (c) Cdc25 PTPs; and (d) low molecular weight PTPs (LMW-PTP) (Tonks, 2013). PTPs have been implicated as important pathogenic and virulence factors for several infectious agents, including viruses, bacteria, fungi and protists (Heneberg, 2012). For instance, a PTP of the enterobacterium *Yersinia pestis* inhibits phagocytosis and the oxidative burst by macrophages (Bahta and Burke, 2012). In kinetoplastid parasites, such as *Trypanosoma* spp. (Gallo et al., 2011; Szoor et al., 2006) and *Leishmania* spp. (Aguirre-García et al., 2006; Nascimento et al., 2006), the PTPs may be involved in the life cycle differentiation and invasion to the host cells. In the protist *Entamoeba histolytica*, two PTPs have been cloned (EhPTPA and EhPTPB) and the up-regulation of EhPTPA may play a role in the adaptive response of the parasite during amoebic liver abscess development (Herrera-Rodríguez et al., 2006).

T. foetus is an extracellular parasite that exerts its cytotoxic effect while interacting with the surfaces of host cells. Therefore, the presence of enzymes with catalytic sites that face the external medium seems to be extremely important for host–parasite interactions. The activities of these enzymes, referred to as ecto-enzymes, can be measured using intact living cells (Cosentino-Gomes and Meyer-Fernandes, 2011; Gomes et al., 2011). In this context, the presence of surface-located phosphatases, called ecto-phosphatases, with high affinity for phosphotyrosine substrates, including non-protein phosphoesters substrates such of *p*-nitrophenyl phosphate (*p*-NPP), has been reported in several pathogenic unicellular microorganisms (Gomes et al., 2011; Heneberg, 2012), including *T. vaginalis* (De Jesus et al., 2002) and *T. foetus* (De Jesus et al., 2006). These enzymes are able to hydrolyse extracellular phosphorylated substrates interfering with some signalising pathways of the host cells (Aguirre-García et al., 2003; Heneberg, 2012). Several biological roles for ecto-phosphatases in protozoa parasites have been suggested, including participation in the processes of proliferation, differentiation, adhesion, virulence, and infection (Cosentino-Gomes and Meyer-Fernandes, 2011; Gomes et al., 2011).

However, little is known about the physiological role of ecto-phosphatase activity in *T. foetus* and there are no reports that provide a characterisation of this ecto-enzyme activity on the EFF. Consequently, in the present study, we characterise the ecto-phosphatase activity on the surface of intact living EFF and compare its biochemical properties to that of the PS. The question of whether a modulation of ecto-phosphatase activity occurs during EFF formation was also assessed. Ultrastructural cytochemistry was performed to localise the enzymatic activity to the parasite surface. To clarify the molecular nature of a part of the ecto-phosphatase activity of EFF, antibodies that recognise different classes of PTPs of *E. histolytica* were assessed using complementary techniques, such as, immunofluorescence, immunogold labelling, immunoblotting and inhibition assays. The possible involvement of the ecto-enzyme activity in the process of EFF transformation and during the interaction of both *T. foetus* forms with epithelial cells was also investigated.

2. Material and methods

2.1. Chemicals

All reagents were purchased from E. Merck (D-6100 Darmsttadt, Germany) or Sigma–Aldrich Chemical Co. (St. Louis, MO). Deionised distilled water was used in the preparation of all solutions.

2.2. Microorganisms and cell culture

2.2.1. T. foetus

The K strain was isolated by Dr. H. Guida (Embrapa, Rio de Janeiro, Brazil) from the genital tract of a bull and has been maintained in culture since the 1970s. The CC09-1 isolate was obtained by Dr. C.M. Campero (Patología Veterinaria, Instituto Nacional de Tecnología Agropecuaria, Balcarce, Argentina) and axenized in 2009. Both strains were cultivated in a trypticase, yeast extract, and maltose (TYM) medium (Diamond, 1957) supplemented with 10% fetal bovine serum. *T. foetus* was grown in Pyrex® culture tubes (O.D. × L: 16 mm × 150 mm), containing 20 mL of TYM medium (initial inoculum: 1×10^4 parasites/mL), for 30 h at 37 °C, which corresponds to the logarithmic growth phase. These isolates are available upon request. The viability of the parasites was checked before and after each assay using the trypan blue dye exclusion method (0.4% in sterile PBS). Based on the ability to destroy MDCK cells, parasites from CC09-1 isolate were previously considered more cytotoxic than those from K strain (Pereira-Neves et al., 2012).

2.2.2. Madin-Darby Canine Kidney (MDCK) cells

The MDCK cells (ATCC Number CCL-34), an epithelial kidney canine cell line, were used in interactions experiments with parasites. The epithelial cells were cultured in 25-cm^2 flasks with DMEM supplemented with 2 mM L-glutamine, 10% heat-inactivated FBS, and 50 μg/mL gentamicin. The cells were kept at 37 °C in 5% CO_2 containing humidified air, with passages every 48 h.

2.3. EFF induction and reversibility assays

To obtain a large number of EFF, cultures of *T. foetus* grown for 30 h at 37 °C in TYM medium were cooled to 4 °C for up to 4 h, without changing the medium during this period. To reversibility assay, some samples were warmed to 37 °C for 4 h after being kept for 4 h at 4 °C. In each assay, the EFF percentage was determined from counts of at least 1000 parasites per sample after several time points using light microscopy. Parasites grown for 30 h under standard conditions were used as controls for both assays. The percentage of PS and EFF was estimated before and after every experimental procedure that was performed throughout this study.

2.4. Preparation of plasma membrane-enriched fraction and marker enzyme assays

PS and EFF (2×10^9 cells) were harvested by centrifugation, washed and resuspended in cold 10 mM Tris–HCl buffer (pH 7.4), containing 0.25 M sucrose, 2 mM $MgCl_2$ and a protease inhibitor cocktail (Sigma – Cat. No. P-2714). The parasites were disrupted with a Potter-type homogeniser on ice and the homogenates were pre-cleared by centrifugation (700×*g* for 10 min at 4 °C). The supernatants (total cell extract) were submitted to three sequential ultracentrifugation steps using a Beckman SW 28 rotor (Beckman Coulter, USA): at 5000×*g* for 15 min, at 12,000×*g* for 30 min and at 100,000×*g* for 60 min. The resultant supernatant (soluble fraction) was stored whereas the pellet (microsome fraction) was resuspended in 10 mM Tris–HCl buffer (pH 7.4), containing 2 mM EDTA, 2 mM DTT, 2 mM $MgCl_2$, 150 mM KCl, 2.2 M sucrose and, subsequently, applied to a discontinuous sucrose gradient (1.0, 1.3, 1.6 and 1.9 M). After centrifugation at 130,000×*g* for 3 h, the band localised at the sample-1.0 M sucrose interface, which was previously characterised as highly enriched in plasma membrane (Díaz et al., 1996) was collected. All procedures were performed at 4 °C. The protein content of each fraction was determined by the Lowry method (Lowry et al., 1951), using BSA as standard.

During cell fractionation, the plasma membrane enrichment was confirmed by detection assays for (Na^+–K^+)-ATPase activity, a classical marker for plasma membrane, and glucose-6-phosphatase activity, a marker enzyme for endoplasmic reticulum. To determine (Na^+–K^+)-ATPase activity, 100 μg of protein of each fraction (stock concentration: 2 mg/mL) were incubated at 30 °C for 1 h in 0.5 mL of a reaction medium containing 20 mM Hepes–Tris (pH 7.0), 10 mM $MgCl_2$, 120 mM NaCl, 30 mM KCl and 5 mM ATP-Na_2 as substrate. After addition of 0.5 mL of cold 25% charcoal in 0.1 M HCl, the reaction tubes were centrifuged at 1500×*g* for 10 min at 4 °C and the supernatants were added to the of Fiske–Subbarow reactive mixture (Fiske and Subbarow, 1925). The rate of inorganic phosphate (Pi) released was then spectrometrically measured at 660 nm wave-length. A Pi curve was used as a standard. The (Na^+–K^+)-ATPase activity was calculated by subtracting the rate of Pi released in the presence of 1 mM ouabain from that obtained in the absence of the inhibitor compound. The glucose-6-phosphatase activity was determined as previously described (Díaz et al., 1996).

2.5. Ecto-phosphatase activity measurements

Phosphatase activity was determined by measuring the rate of *p*-nitrophenol (*p*-NP) production from the hydrolysis of *p*-NPP. PS and EFF were harvested by centrifugation, washed three times and kept in A-buffer (116.0 mM NaCl, 5.4 mM KCl, 5.5 mM D-glucose and 50 mM Hepes–Tris buffer, pH 7.2). Afterwards, intact living PS and EFF (1×10^7 cells/mL) or 100 μg of protein of membrane fractions were incubated at 25 °C for 40 min in 0.5 mL of a reaction medium containing A-buffer and 5 mM *p*-NPP as a substrate. After addition of 1 mL of 1 N NaOH, the reaction tubes were centrifuged at 1500×*g* for 10 min at 4 °C and the supernatants were measured with a spectrophotometer at 425 nm wave-length. A *p*-NP curve was used as a standard. The phosphatase activity was calculated by subtracting the non-specific *p*-NPP hydrolysis measured in the absence of parasites. The rate of ecto-phosphatase activity was expressed as nmol of *p*-NP released per hour per 10^7 cells.

2.6. Secreted phosphatase measurements

The supernatants from *T. foetus* cultures (PS and EFF) were collected by centrifugation and filtered using 0.22 μm membranes. Meanwhile, the PS and EFF (1×10^7 cells/mL) were washed and incubated in A-buffer for 40 min at 25 °C. Afterwards, these supernatants were also collected and filtered as outlined above. The absence of parasites in the TYM medium or A-buffer supernatants was confirmed using light microscopy. The enzymatic reaction was performed and measured, as described in the Section 2.5.

2.7. Inhibition assays

Several concentrations of inhibitors sodium orthovanadate (SO), ammonium molybdate (AM), sodium fluoride (NaF) and Pi were added to the enzymatic reaction medium. In some assays, the polyclonal anti-amoebic acid PTPs antibodies, mentioned in the Section 2.8, were added to the reaction medium. Afterwards, the *p*-NPP hydrolysis was measured, as described in the Section 2.5. The ecto-phosphatase activities in the absence of inhibitors were assumed to be 100%. To assess inhibitor reversibility, the PS and EFF (1×10^7 cells/mL) were pre-incubated in A-buffer containing 100 μM SO, AM, NaF and 10 mM Pi or the anti-amoebic PTPs antibodies. After 30 min at 25 °C, the parasites were washed and the *p*-NP production was determined, as mentioned above. As control, the parasites were pre-incubated in A-buffer without inhibitors.

2.8. Immunofluorescence

PS and EFF were fixed with paraformaldehyde and allowed to adhere to poly-L-lysine-coated glass coverslips. The parasites (permeabilized or not with 0.1% Triton X-100 for 10 min) were blocked with 50 mM ammonium chloride and 3% BSA. In some assays, the non-permeabilized parasites were treated with 5% urea in 0.1 M Tris–HCl (pH 9.5) at 90 °C for 5 min before blocking. Next, the samples were incubated overnight at 4 °C with the following polyclonal anti-amoebic acid PTPs antibodies: (a) anti-EhPTPA or anti-EhPTPB (dilution 1:100) generated against two classical PTPs (Herrera-Rodríguez et al., 2006); and (b) anti-EhPRL (dilution 1:200) raised against a dual specificity PTP (GenBank accession number: XP_657240.1) similar to phosphatase of regenerating liver (PRL) (Ramírez-Tapia et al., 2013). The preimmune serum was used as negative control. The primary antibodies were revealed with an anti-mouse IgG Alexa-488-conjugated antibody (Life Technologies, USA), and the samples were observed using a Zeiss Axiophot II fluorescent microscope (Zeiss, Germany). The images were randomly acquired with a high resolution digital camera (AxioCam MRc5, Zeiss, Germany). In some assays, the primary antibodies were omitted and the samples were incubated with the anti-mouse Alexa-488-conjugated antibody only. No labelling was observed under this condition.

2.9. Transmission electron microscopy (TEM)

2.9.1. Ultrastructural cytochemistry for ecto-phosphatase activity

To localise the phosphatase activity on the parasite surface, both forms were prefixed in 1% glutaraldehyde in 0.1 M cacodylate buffer (pH 7.2) for 30 min at 25 °C. Afterwards, the parasites were incubated for 60 min at 25 °C in a reaction medium containing 0.1 M Tris–maleate buffer (pH 6.8), 10 mM *p*-NPP and 2.4 mM lead nitrate. The parasites were re-fixed in 2.5% glutaraldehyde in 0.1 M cacodylate buffer (pH 7.2) for 2 h at 25 °C, post-fixed for 30 min in 1% OsO_4, dehydrated in acetone and embedded in Epon. As controls, the parasites were incubated either in the absence of *p*-NPP or in the presence of 100 μM SO. Ultrathin sections were observed with a JEOL 1210 transmission electron microscope. The images were randomly acquired with a CCD camera system (MegaView G2, Olympus, Germany).

2.9.2. Immunogold electron microscopy

PS and EFF were processed for TEM, as described above. For immunolabelling, thin sections were etched with 0.1% hydrogen peroxide for 10 min and quenched in 50 mM ammonium chloride, 3% and 1% BSA, and 0.2% Tween-20. Next, the samples were incubated with the anti-amoebic PTPs antibodies or the preimmune serum, as described in the Section 2.8. After several washes, the thin sections were incubated with 10 nm gold-labelled goat anti-mouse IgG (BB International, UK) and observed as mentioned above. In some assays, the primary antibodies were omitted and the samples were incubated with the gold-labelled goat anti-mouse antibody only. No labelling was observed under this condition.

2.10. Immunoblotting

Samples of the total cellular extract (20 μg) or of the membrane fractions (20 μg) from PS and EFF were separated by 12% SDS–PAGE and transferred to a polyvinylidene fluoride (PVDF) membrane (Millipore Corporation, USA). Kaleidoscope Pre-stained Standard (Bio-Rad, Brazil) was used as molecular weight standard. Blots were incubated with the anti-EhPRL antibody (dilution 1:2000) for overnight at 4 °C. The preimmune serum was used as negative control. The specifically bound primary antibodies were detected using a horseradish peroxidase-conjugated goat anti-mouse IgG antibody (dilution1:2000) for 1 h at room temperature. Blots were developed using the DAB Enhanced Liquid Substrate system (Sigma–Aldrich Chemical Co., St. Louis, MO), according the manufacturer's instructions. The images were acquired with a scanner (HP G4050, Hewlett–Packard, Brazil). A mouse polyclonal anti-GAPDH antibody (dilution 1:1000) was used as loading control for the samples from the total cellular extract. For the loading control, the same samples were loaded in separated slots on the same gel for EhPRL labelling and, posteriorly, the gel was cut and blotted in a separated PVDF membrane. The protein levels were quantified by densitometry analyses using GelQuantNET software (http://biochemlabsolutions.com/GelQuantNET.html) and were expressed in relative densitometry units. The results were normalised to the intensity of GAPDH bands for each corresponding sample. We did not find available antibodies that specifically recognise proteins in the samples of the plasma membrane fraction from *T. foetus* to be used as a proper loading control.

2.11. Effects of SO and anti-amoebic PTPs antibodies on EFF induction and reversibility assays

PS and EFF were pre-incubated for 30 min at 25 °C in A-buffer containing either 100 μM SO or the anti-amoebic PTPs antibodies. As control, both forms were pre-incubated in A-buffer without inhibitor or antibodies. The preimmune serum was also used as negative control. Afterwards, untreated or pre-treated parasites with SO or anti-PTPs antibodies, were washed, kept in A-buffer and submitted to the EFF induction and reversibility assays, as outlined in the Section 2.3. To determine whether SO or anti-PTPs antibodies were able to induce EFF formation, pre-treated parasites with SO or anti-PTPs antibodies were washed and kept in A-buffer for up to 4 h at 25 °C.

2.12. Parasite–host cell interactions

All conditions for the co-incubation assays were exactly the same as those established in a previous study (Pereira-Neves et al., 2012). MDCK cells were seeded onto 24-well tissue culture plates in DMEM medium and allowed to form a confluent monolayer (2×10^5 cells) at 37 °C in 5% CO_2. Confluent MCDK cells were co-incubated with either the PS or the EFF for 1.5 h at a parasite to host cell ratio of 5:1. As control, parasites were not added to monolayers. The interaction assay was monitored by inverted phase-contrast microscopy. The percentage of PS and EFF in each sample and the average number of attached parasites per microscopic field were determined. After co-incubation, MTT assay was performed as previously described (Pereira-Neves et al., 2012), to compare the cytotoxicity of both forms to MDCK cells. The cytotoxicity was calculated with the following equation: $1 - (E/C)$. All measurements of experimental (E) samples were indexed to those of control (C) samples (E/C), which showed no loss of viability, and then subtracted from 1.0. In some samples, prior to co-incubation assays, both forms were pre-incubated with SO or the anti-amoebic PTPs antibodies, as described in the Section 2.11. Afterwards, untreated or pre-treated parasites were used immediately for interaction assays with MDCK cells, as outlined above.

2.13. Statistical analysis

Statistical comparison was performed by two-way ANOVA test, using computer analysis (GraphPad Prism v. 5.00, California, USA). $p < 0.05$ was considered to be statistically significant. The kinetic parameters, maximal velocity (V_{max}) and apparent Michaelis–Menten constant (K_m), for *p*-NPP were calculated using a computerised non-linear regression analysis of the data to the Michaelis–Menten

equation (GraphPad Prism v. 5.00, California, USA). The results for all assays are the average of three independent experiments performed at least in triplicate.

3. Results

3.1. Ecto-phosphatase activity

3.1.1. Establishment of conditions for the enzymatic assays

The experiments were performed using intact living PS and EFF obtained from a low- (K) and a high- (CC09-1) cytotoxic strain. The results for the EFF induction and reversibility assays obtained here were exactly the same as those previously reported (Pereira-Neves and Benchimol, 2009; Pereira-Neves et al., 2012). Parasites exhibiting a PS or amoeboid body with at least one visible external flagellum were designated as PS (Supplementary Fig. S1a). Only parasites with no visible external flagella were considered to be EFF (Supplementary Fig. S1b, c). Preliminary experiments were performed to establish the optimal conditions for minimising the reversion rate of the EFF and for avoiding the transformation of PS into EFF during the enzymatic assays. After these experiments, the ecto-phosphatase activities for both forms were measured for 40 min at 25 °C in A-buffer containing *p*-NPP. Unless otherwise specified, under all conditions used throughout the present work, the number of parasite per mL, the cell viability and the percentage of the PS and EFF in each sample remained unaltered.

Some assays were performed using a plasma membrane-enriched fraction of PS and EFF. In this fraction, the activity of the plasma membrane marker enzyme (Na^+–K^+)-dependent, ouabain-sensitive ATPase was ~11-fold greater than that of the total cell extract (Supplementary Fig. S2). The low activity of glucose-6-phosphatase detected in the plasma membrane fraction indicated that the contamination by endoplasmic reticulum was minimal (Supplementary Fig. S2). These results were similar for both forms and isolates.

3.1.2. Biochemical properties of ecto-phosphatase activities in PS and EFF T. foetus

The intact living PS from K (Fig. 1a) and CC09-1 (Fig. 1b) strains hydrolysed the phosphotyrosine analogue *p*-NPP at a rate of 13.15 ± 0.77 and 59.09 ± 4.24 nmol *p*-NP.10^{-7} cells h^{-1}, respectively, at pH 7.2. The phosphatase activities of living EFF from K and CC09-1 strains were ~5.0- and 1.6-fold greater than those of PS, respectively (Fig. 1a, b) ($p < 0.001$). In both strains, the phosphatase activities of PS and EFF were linear for at least 60 min and with the increase of parasite density (Supplementary Fig. S3).

To determine whether *p*-NPP hydrolysis was a consequence of enzyme secretion or cellular lyses, PS and EFF were incubated in A-buffer without *p*-NPP and these supernatants, as well those from the TYM culture medium were assessed for phosphatase activity (Fig. 1a, b). The supernatants of either TYM or A-buffer from both forms exhibited, respectively, less than 10% and 2% of the phosphatase activities that were found using living parasites (Fig. 1a, b). These results ruled out the possibility that the phosphatase activities could be derived from either lysed parasites or from phosphatases that had been secreted into the reaction medium.

To analyse the influence of pH, the ecto-phosphatase activities of intact living PS and EFF were measured in a pH range from 6.4 to 8.0 (Fig. 2a, b). This range was chosen because the viability of both forms was decreased at a pH lower than 6.0 or higher than 8.0 and ~30% of PS was transformed into EFF after 30 min of incubation in A-buffer at a pH range of 6.0–6.3. The ecto-enzyme activities of living PS and EFF were decreased as the pH was increased, suggesting the presence of acid phosphatase activities (Fig. 2a, b). Using a plasma membrane-enriched fraction of PS and EFF, it was found that the ecto-phosphatase activities of PS and EFF reached a maximum at pH 6.4 and 6.0, respectively (Fig. 2c, d). The ecto-enzyme activities of living (Fig. 2a, b) and membrane fraction (Fig. 2c, d) of EFF were significantly higher than those in PS within the pH range of 6.4–7.6 and 6.0–7.6, respectively. At each pH value in these ranges, PS and EFF from the CC09-1 isolate (Fig. 2b, d) exhibited higher ecto-phosphatase activities when

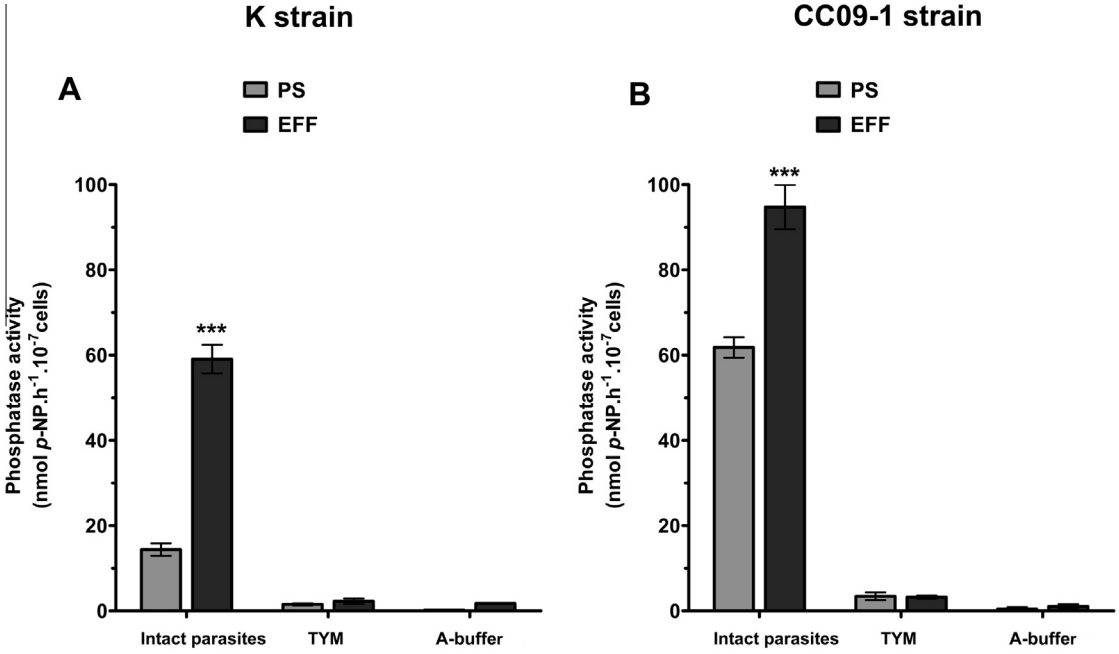

Fig. 1. Detection of phosphatase activity in intact living parasites and in the supernatants of TYM culture and A-buffer medium from PS (light grey bars) and EFF (dark grey bars). (a) K strain. (b) CC09-1 isolate. The values are expressed as the means ± S.D of three independent experiments, each performed in triplicate. The enzyme reactions were performed at pH 7.2. In both strains, the phosphatase activities of EFF were greater than those of PS. The supernatants of both TYM and A-buffer medium from both forms failed to show *p*-NPP hydrolysis. ***$p < 0.001$ compared with PS.

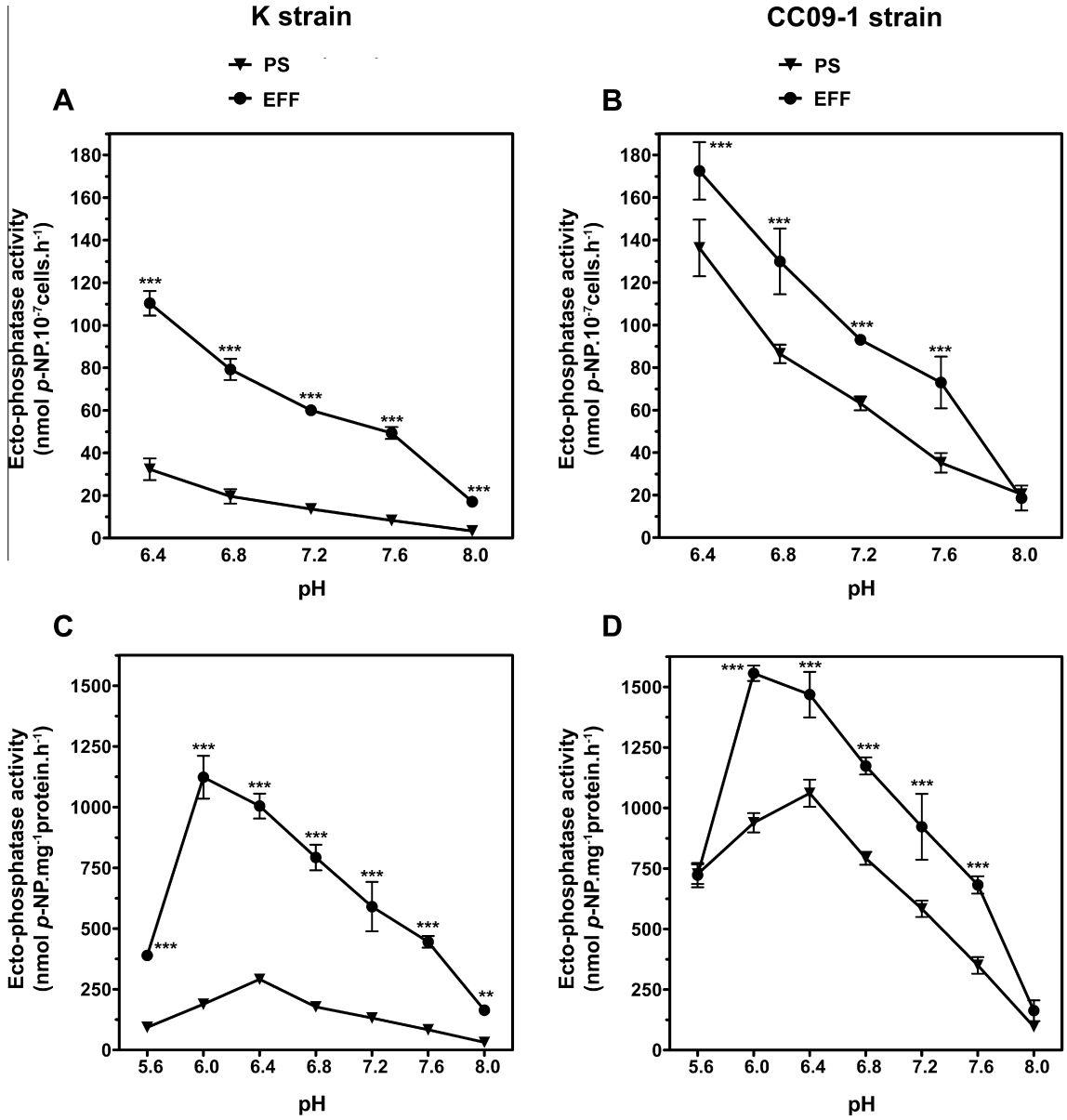

Fig. 2. Influence of pH on the ecto-phosphatase activities of intact living (a, b) and plasma membrane-enriched fraction (c, d) of PS (▼) and EFF (●) from K (left-hand panels) and CC09-1 strains (right-hand panels). The values are expressed as the means ± S.D of three independent experiments, each performed in triplicate. In both strains, the ecto-phosphatase activities of PS and EFF reached a maximum at pH 6.4 and 6.0, respectively. The ecto-enzyme activities of living and membrane fraction of EFF were higher than those of PS at a pH range of 6.4–7.6 and 6.0–7.6 respectively. $^{**}p < 0.01$; $^{***}p < 0.001$ compared to PS.

Table 1
Kinetic parameters of ecto-phosphatase activities detected on living PS and EFF *T. foetus*.

Kinetic parameters	K strain		CC09-1 strain	
	PS	EFF	PS	EFF
V_{max} (nmol *p*-NP.10^{-7} cells h^{-1})	19.09 ± 0.39	63.80 ± 1.12	64.37 ± 1.04	101.50 ± 1.63
K_m (mM *p*-NPP)	1.93 ± 0.15	0.60 ± 0.05	0.60 ± 0.05	0.57 ± 0.05

Note: The individual V_{max} and K_m values were obtained by non-linear regression using the Michaelis–Menten equation. The enzyme reactions were performed at pH 7.2. The values are expressed as the means ± S.D of three independent experiments, each performed in triplicate.

compared to those from the K strain (Fig. 2a, c), respectively. Although the enzymatic activities exhibited an optimum pH in the acidic range, all experiments were carried out at pH 7.2 because the lowest EFF reversion rates were obtained at this pH for incubations longer than 60 min in A-buffer.

The dependence on *p*-NPP concentration revealed a normal Michaelis–Menten kinetics for the ecto-phosphatase activities of intact living PS and EFF (Supplementary Fig. S4). The comparison of the kinetics parameters obtained for the PS and EFF from K and CC09-1 strains suggests that the ecto-phosphatase activities could

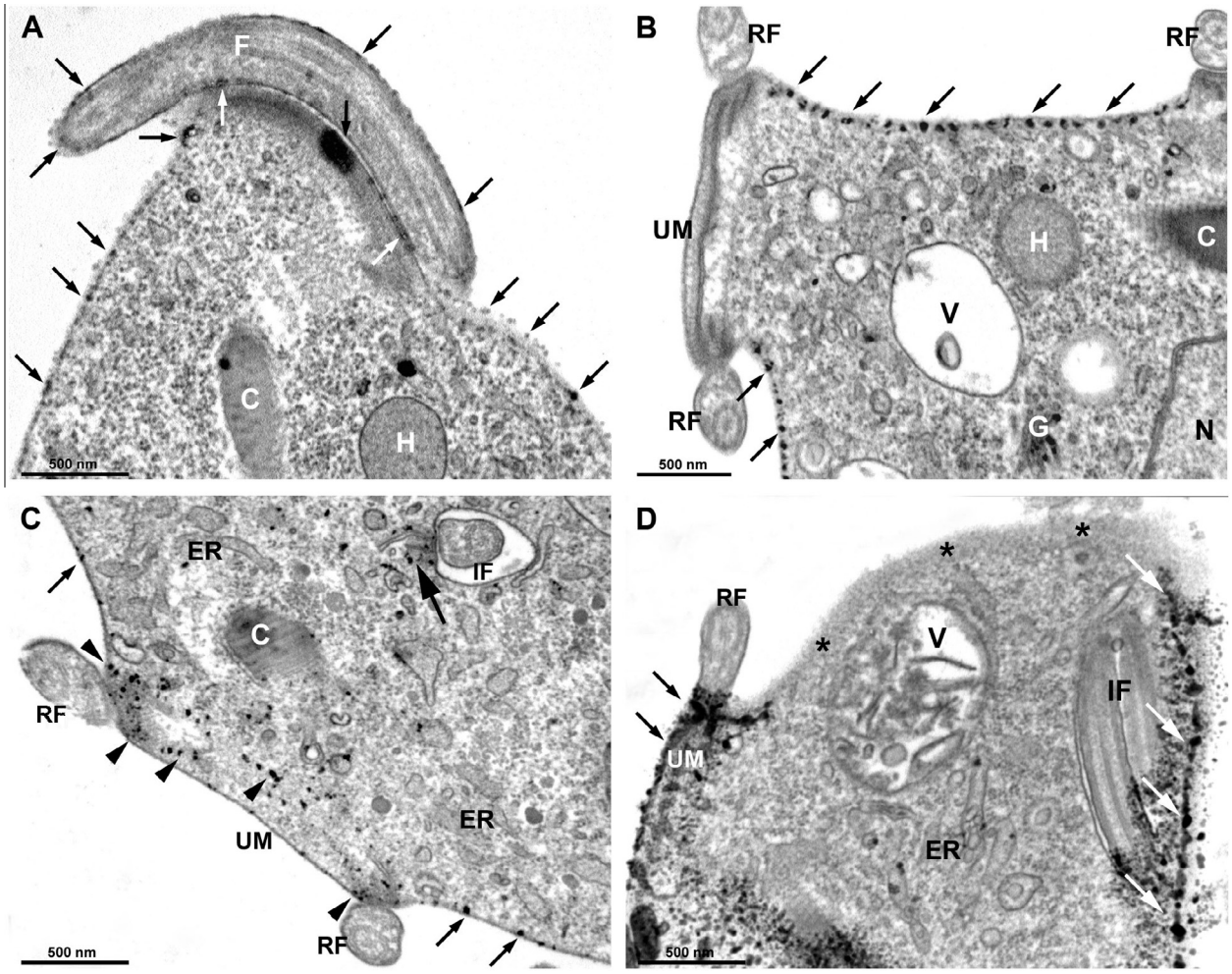

Fig. 3. Ultrastructural cytochemistry for phosphatase activity in PS from the CC09-1 isolate grown under standard conditions (a,b) and parasites undergoing the process of EFF transformation (c,d). (a,b) A positive labelling (arrows) is seen homogeneously distributed on the external surface and the anterior flagella (F). (b) No labelling is observed on the recurrent flagellum (RF) surface and the undulating membrane (UM). (c,d) Parasites at 4 °C for 1 h. Some regions of flagella are internalised (IF), whereas regions of RF are still external. (c) Labelling is homogeneously seen on the UM (arrow heads), cell surface (small arrows) and the internalised undulating membrane (large arrow). (d) The enzymatic activity is observed on the UM (black arrows) and cell surface (white arrows). Some regions of plasma membrane (asterisks) are not labelled. C, costa; ER, endoplasmic reticulum; H, hydrogenosome; V, vesicle. Bars, 500 nm.

be distinct in the two forms and also between both isolates (Table 1). The phosphatase activity of PS from the K strain presented low capacity (V_{max} value) and affinity (K_m value) for the *p*-NPP, whereas the EFF from the same strain and both forms from the CC09-1 isolate exhibited enzyme activities with higher capacity and affinity for the substrate (Table 1). Although the enzymatic activities of PS and EFF from the CC09-1 strain have shown similar affinity for the *p*-NPP, the EFF presented a higher enzyme capacity when compared to the PS (Table 1).

To further characterise and compare the phosphatase activities of both forms, the effects of several phosphatase inhibitors on *p*-NPP hydrolysis were investigated. AM (Supplementary Fig. S5a, b) and SO (Supplementary Fig. S5c, d), two well-known inhibitors of acid PTPs, and NaF (Supplementary Fig. S5e, f), an inhibitor of acid phosphatases, reduced the phosphatase activities of living PS and EFF in a dose-dependent manner. In the K strain, the ecto-phosphatase activity of the EFF was more susceptible to these compounds when compared to the PS ($p < 0.001$); however, there was no significant difference between the enzyme inhibition profiles of EFF from both isolates and PS from the CC09-1 strain (Supplementary Fig. S5a, f). Similar results were obtained when the enzymatic assays were performed using plasma membrane-enriched fractions (Supplementary Table S2). These data suggest the presence of distinct ecto-phosphatase activities between both forms, at least in the K strain. Pi, the final product of enzyme reactions catalysed by phosphatases, provoked a similar pattern of enzyme inhibition in living PS and EFF from both isolates (Supplementary Fig. S5g, h).

Levamizole (up to 1.0 mM), a well-known alkaline phosphatase inhibitor, sodium tartrate (up to 1.0 mM), an inhibitor for secreted phosphatases, okadaic acid (up to 10 μM) and microcystin-LR (up to 100 nM), two specific phosphoserine/threonine phosphatase inhibitors, had no significant effects on the phosphatase activities of living PS and EFF from both isolates (Supplementary Table S1). In addition, the impermeant anion channel blocker 4,4′-diisothiocyanatostilbene-2,2′-disulfonic acid (DIDS) (up to 1.0 mM) and ouabain (up to 1.0 mM), a Na^+/K^+-ATPase inhibitor, were also tested to rule out the influence of anion transporters and surface ATPases on the phosphatase activities of both forms. These two compounds did not affect the enzyme activities of PS and EFF from both isolates (Supplementary Table S1).

Only SO showed an irreversible effect on the ecto-phosphatase activities of both living forms. Taken together, these results suggest

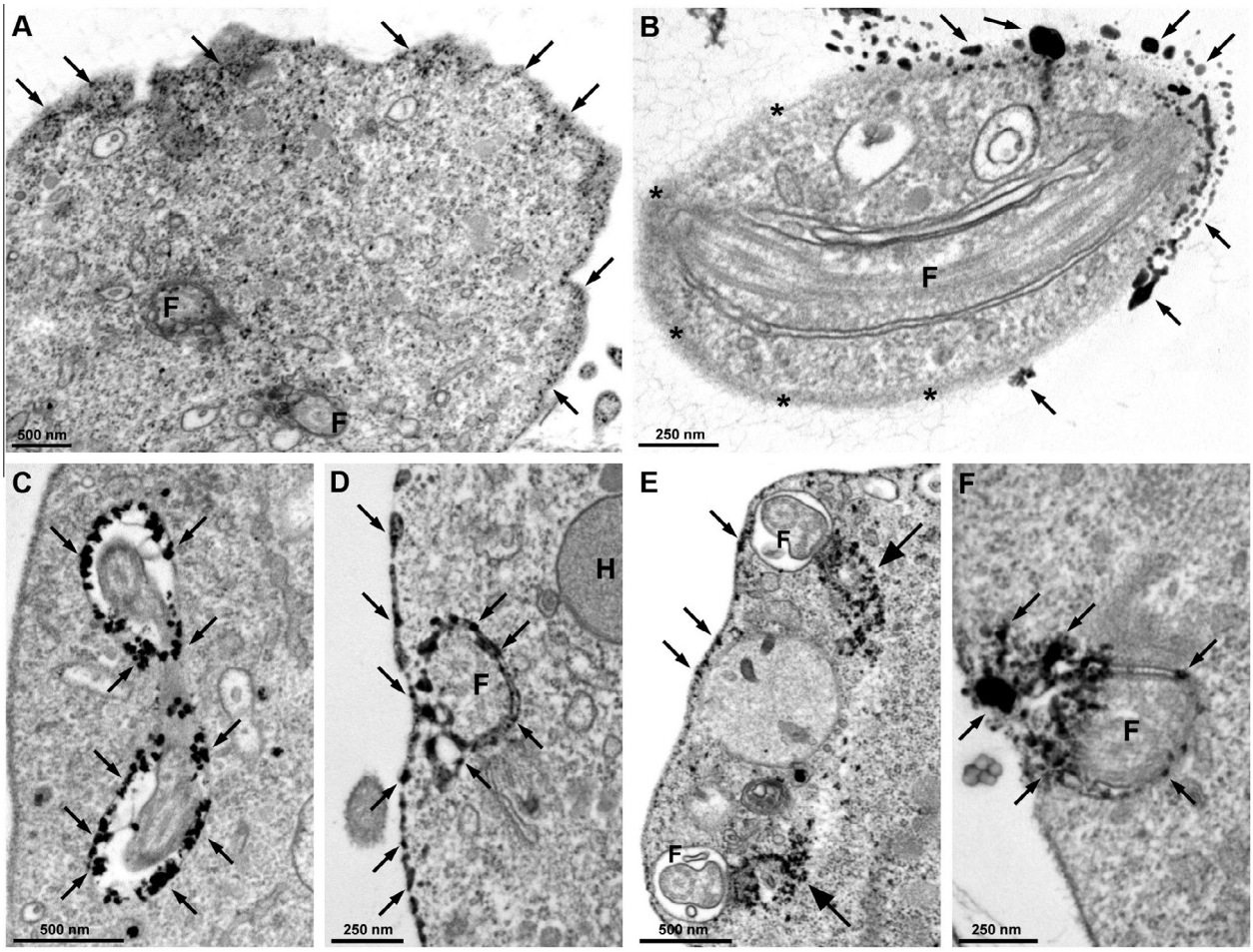

Fig. 4. Ultrastructural cytochemistry for phosphatase activity in EFF from the CC09-1 strain obtained after induction assay. Notice that flagella (F) are internalised. (a) Labelling (arrows) is homogeneously seen on the cell surface. (b) Large electron-dense precipitates (arrows) are heterogeneously observed on the cell surface. Some regions of the plasma membrane (asterisks) are not labelled. (c,d) A labelling (arrows) is observed on the cytoplasmic flagellar canal and plasma membrane. (e) The parasite is labelled on the cell surface (small arrows) and in the internalised undulating membrane (large arrow). (f) The enzymatic activity (arrows) is seen on the surface regions where the flagella (F) were internalised. H, hydrogenosomes. Bars, a, c, e 500 nm; b, d, f 250 nm.

that the ecto-enzyme activities of PS and EFF exhibited similar characteristics of the acid PTP.

3.1.3. Ultrastructural cytochemistry for ecto-phosphatase activity

To localise the ecto-phosphatase activity in the EFF and compare its distribution to that on the PS, ultrastructural cytochemistry was performed (Figs. 3 and 4). Similar results were obtained for both isolates: ~100% of PS ($n = 3$, 100 ultra-thin sections) exhibited small electron-dense deposits homogeneously distributed on their surfaces (Fig. 3a,b), including the anterior flagellar membranes (Fig. 3a). However, no reaction was found on the recurrent flagellum surface and the undulating membrane (Fig. 3b). In contrast, the undulating membranes of parasites undergoing the EFF transformation were labelled (Fig. 3c,d) and ~77% of the parasites ($n = 3$, 100 ultra-thin sections) exhibited small electron-dense deposits homogeneously distributed on the undulating membrane and cell surface (Fig. 3c), whereas ~23% presented large electron-dense clusters homogeneously distributed on the undulating membrane but heterogeneously found on the plasma membrane (Fig. 3d).

After the induction assay, the external surface of the EFF exhibited a labelling similar to that observed in parasites undergoing EFF transformation (Fig. 4a,b). The plasma membranes of ~60% of EFF ($n = 3$, 100 ultra-thin sections) presented small deposits that were homogeneously distributed (Fig. 4a), whereas large electron-dense precipitates were heterogeneously found on the surfaces of ~40% (Fig. 4b). In all analyses, the EFF also exhibited a labelling on the cytoplasmic flagellar canals (Fig. 4c,d), in the internalised undulating membranes (Fig. 4e) and on the surface regions where the flagella were internalised (Fig. 4f). After the reversibility assay, the distribution pattern of the ecto-phosphatase activity was similar than that found in PS before EFF induction (not shown). In both forms, the controls presented negative results (not shown).

3.2. Time-course of ecto-phosphatase activity during EFF induction and reversibility assays

The differential distribution of ecto-phosphatase activities between PS and EFF, as detected by cytochemistry, led us to assess whether a modulation of enzyme activity occurs during the EFF transformation. A positive correlation between ecto-phosphatase activity and EFF formation was observed (Fig. 5). In both isolates, an increase in the percentage of the EFF resulted in a proportional increase in ecto-phosphatase activity (Fig. 5a,b). During the reversibility assay, the percentage of the EFF and the enzyme activity decreased and were restored to the levels found in PS before EFF induction (Fig. 5c,d).

3.3. Immunodetection assays for PTPs

Because the ecto-phosphatase activities of PS and EFF exhibited similar characteristics of PTP, immunodetection assays with three

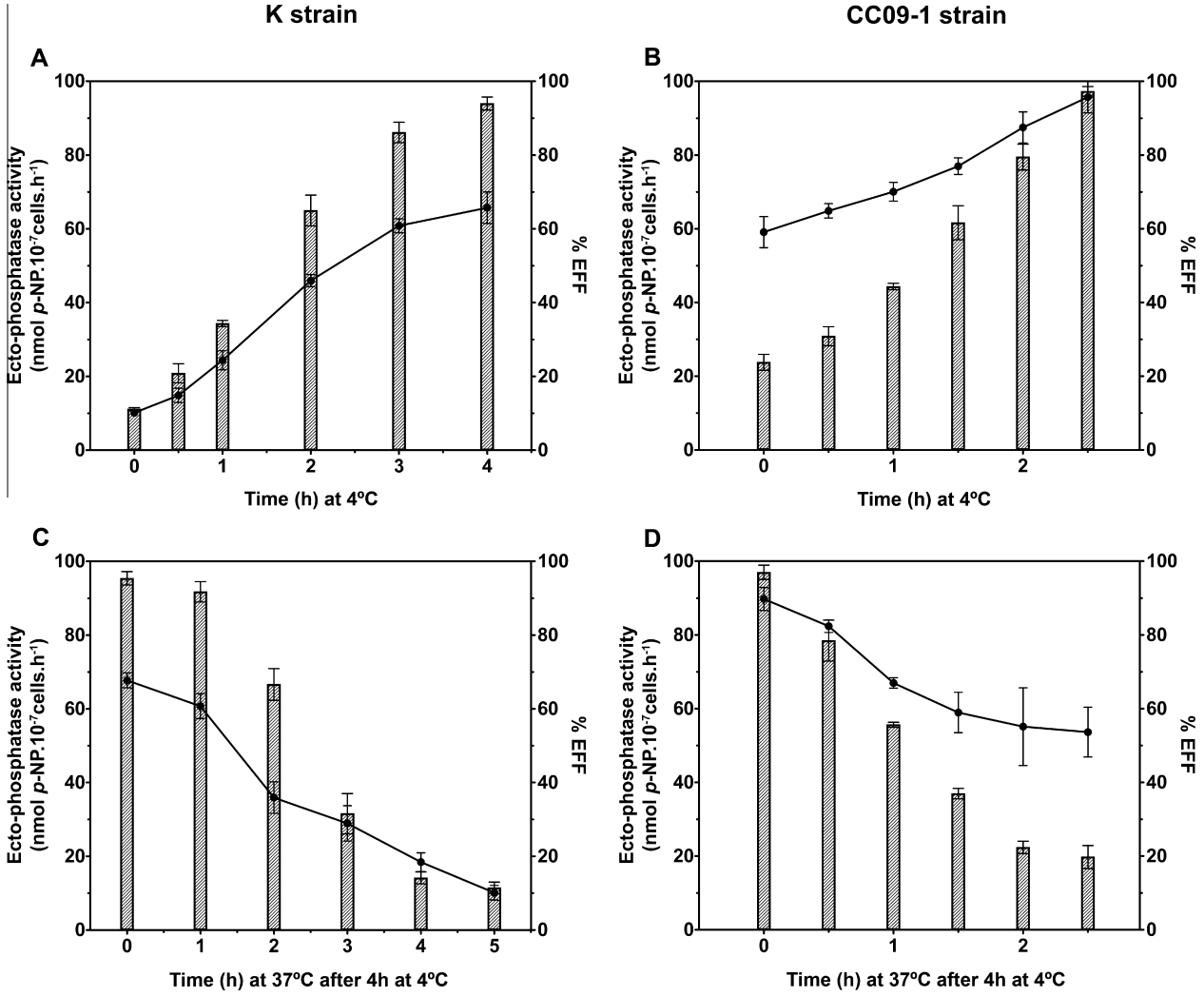

Fig. 5. Time course of ecto-phosphatase activity in living parasites from the K (left-hand panels) and CC09-1 isolates (right-hand panels) during EFF induction (a,b) and reversibility (c,d) assays. The values are expressed as the means ± S.D of three independent experiments, each performed in triplicate. The enzyme reactions were performed at pH 7.2. (a,b) In both isolates, the ecto-phosphatase activities (■) increased over the course of EFF induction (columns). (c,d) During the course of EFF reversibility (columns), the ecto-phosphatase activities (■) of both isolates decreased and were restored to the levels found in PS before EFF induction.

polyclonal antibodies that recognise two different groups of PTPs of *E. histolytica* were performed in attempt to better clarify the molecular nature of a part of the ecto-enzyme activities of both parasite forms, at least. Initially, the antibodies were assessed by immunofluorescence in order to determine which of them were able to recognise the parasite's surface. Non-permeabilized and permeamilized PS and EFF were used. In all conditions, no labelling was observed when anti-EhPTPA and anti-EhPTPB antibodies (generated against two classical PTPs) were used (not shown).

In contrast, the labelling obtained with anti-EhPRL antibody (raised against a dual specificity PTP similar to PRL) showed promising results (Fig. 6). In the K strain, non-permeabilized PS did not exhibit labelling (Fig. 6a,b), whereas both spontaneous EFF (Fig. 6a,b), which are naturally encountered under standard growth conditions, and EFF obtained after cold-induction assay (Fig. 6c,d) showed a strong staining on the cell surface. In the CC09-1 isolate, both PS (Fig. 6e,f) and EFF (spontaneous and cold-induced) (Fig. 6e,h) presented a surface labelling; however, the intensity of staining on EFF was higher than that observed on PS (Fig. 6e,h). In permeabilized PS an EFF from both strains, the labelling of anti-EhPRL antibody was found as punctate cytoplasmic structures and in the perinuclear region (Supplementary Fig. S6). No fluorescence was observed when the preimmune serum was used (not shown). No changes were observed in the labelling pattern when non-permeabilized PS and EFF were submitted to the heat-induced epitope retrieval treatment (not shown).

Immunoelectron microscopy confirmed a labelling on the plasma membrane of PS from CC09-1 isolate and EFF from both strains (Supplementary Fig. S7). PS and EFF from both isolates also presented a labelling in the endoplasmic reticulum, Golgi complex and on the surface of vesicles that were found close to the plasma membrane and throughout the cytosol (Supplementary Fig. S7).

Immunoblotting revealed that the anti-EhPRL antibody specifically cross-reacted with a 24-kDa protein of PF and EFF from both isolates (Fig. 7; Supplementary Fig. S8). In the total extract fractions of both strains, the expression level of 24-kDa protein increased ~1.4-fold after EFF induction (Supplementary Fig. S8b). However, in the plasma membrane-enriched fraction, the 24-kDa protein levels in EFF from K and CC09-1 strains were ~4.7- and 1.6-fold greater than those of PS, respectively (Fig. 7). In each

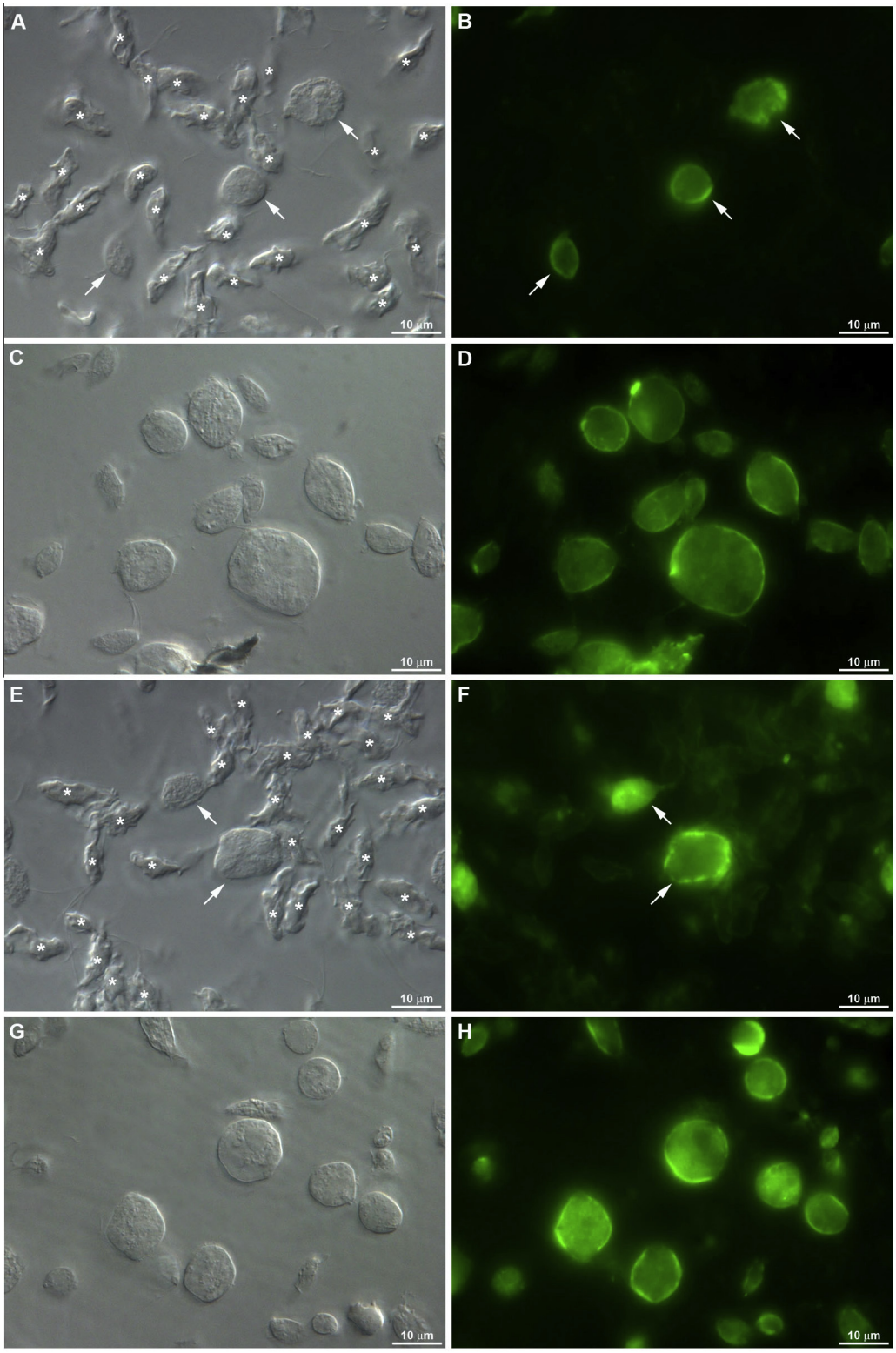

Fig. 6. Immunofluorescence of non-permeabilized PS and EFF after incubation with anti-EhPRL antibody. Left-hand panels: DIC microscopy; Right-hand panels: fluorescence microscopy. (a,b) Parasites from K strain under standard culture conditions. No labelling is observed in PS (asterisks). Spontaneous EFF (arrows) exhibit an intense surface labelling. (c,d) EEF from K strain obtained after induction assay showing cell surface staining. (e,f) Parasites from CC09-1 isolate under standard growth conditions. PS (asterisks) exhibit a moderate surface staining and spontaneous EFF (arrows) show a more intense labelling. (g,h) EEF from CC09-1 isolate obtained after induction assay exhibiting cell surface labelling. The images (b,d) and (f,h) were acquired with 310 ms and 198 ms exposure time, respectively. Bars, 10 µm.

strain, the ratio of the 24-kDa protein expression in the plasma membrane of PS and EFF (Fig. 7) was similar to the ratio of the ecto-phosphatase activities obtained for PS and EFF at pH 7.2 (Figs. 1 and 2). No significant differences were found in the 24-kDa protein levels of EFF from K strain and PS from CC09-1 isolate (Fig. 7; Supplementary Fig. S8).

To verify whether a reorganisation in the surface-labelling pattern of the anti-EhPRL antibody occurs during the EFF

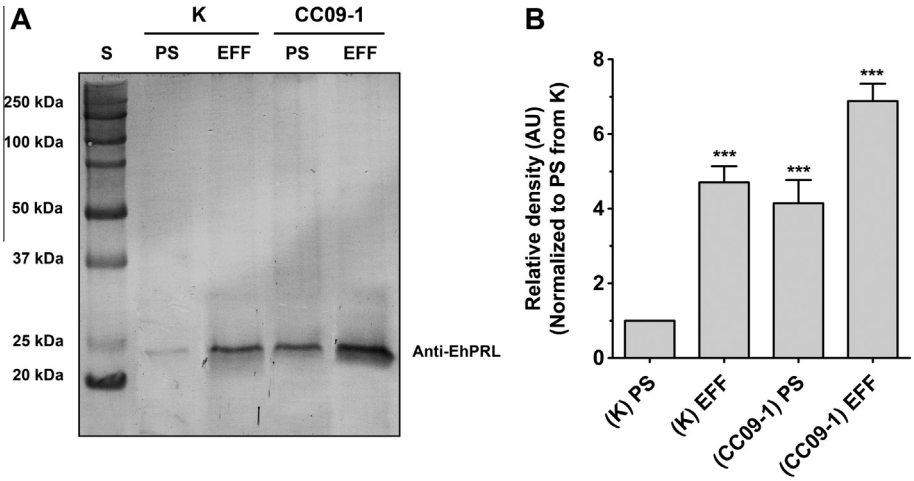

Fig. 7. Immunoblot analyses of anti-EhPRL antibody in the plasma membrane-enriched fractions of PS and EFF from K and CC09-1 strains. (a) Representative immunoblot showing that the antibody reacted specifically with a 24-kDa protein. S, molecular weight standard. (b) Densitometric analysis. The results are normalised to the intensity of bands of PS from K strain and are expressed as relative density in arbitrary units (AU) ± S.D of three independent experiments. The 24-kDa protein levels increased ~4.7- and 1.6-fold after EFF induction in K and CC09-1 strains, respectively. $^{***}p < 0.001$ compared to PS from K strain.

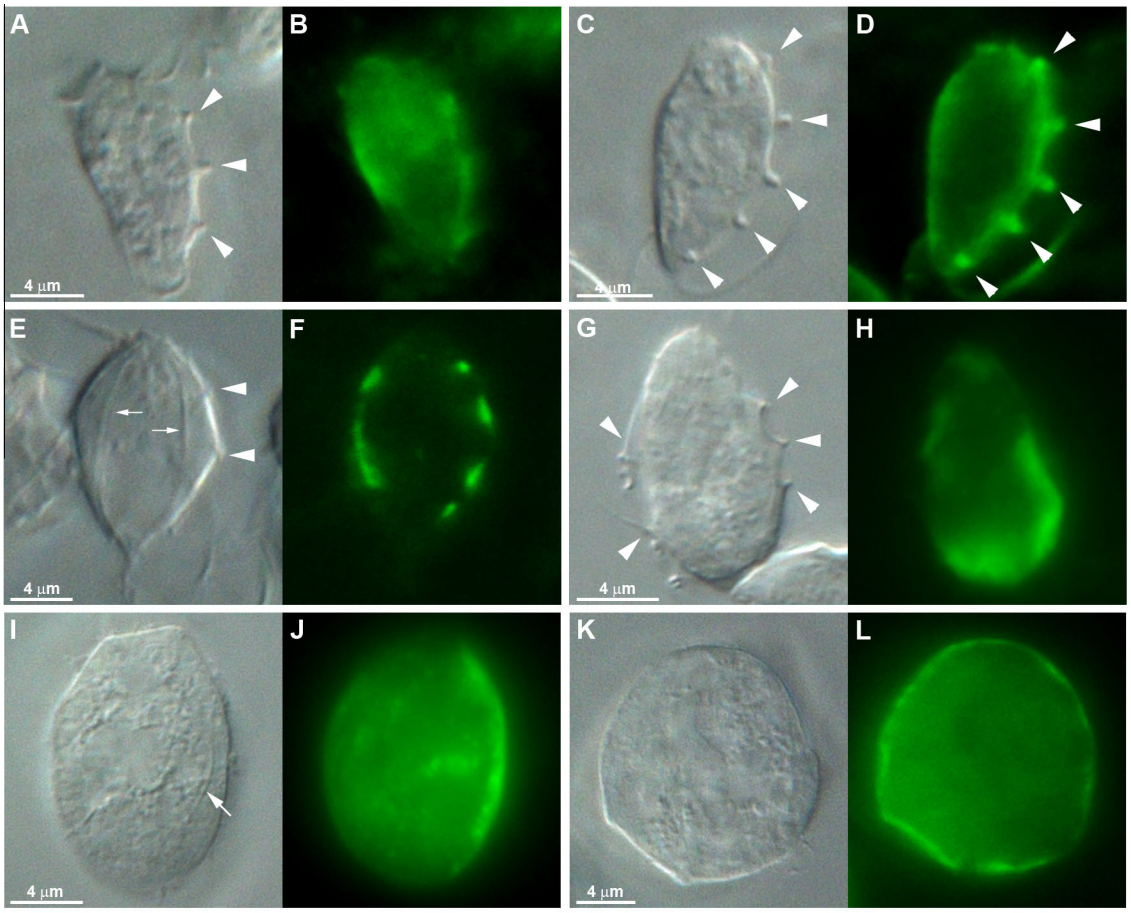

Fig. 8. DIC microscopy followed by immunofluorescence of non-permeabilized parasites during the EFF transformation using the polyclonal anti-EhPRL antibody. (a,b) PS from CC09-1 strain under standard growth conditions. No labelling is observed on the recurrent flagellum and the undulating membrane (arrowheads). (c,d) PS from CC09-1 strain after 30 min at 4 °C. A labelling is homogeneously seen on the cell surface and undulating membrane (arrowheads). (e,f) PS from K strain after 30 min at 4 °C. A labelling is observed in a patchwork pattern on the adjacent surface area to the recurrent flagellum (arrowheads) and costa (arrows), a cytoskeletal structure associated to this flagellum. (g,h) PS from K strain after 1 h at 4 °C. A labelling is heterogeneously seen along the parasites' surface with higher fluorescence intensity on the adjacent region to the recurrent flagellum (arrowheads). (i–l) EFF from CC09-1 strain obtained after induction assay. (i,j) A labelling is observed in a patchwork pattern on the adjacent surface to the costa (arrows). (k,l) A homogeneous staining is seen on the parasite's surface. The images (b,d,f,h) and (j,l) were acquired with 310 ms and 198 ms exposure time, respectively. Bars, 4 μm.

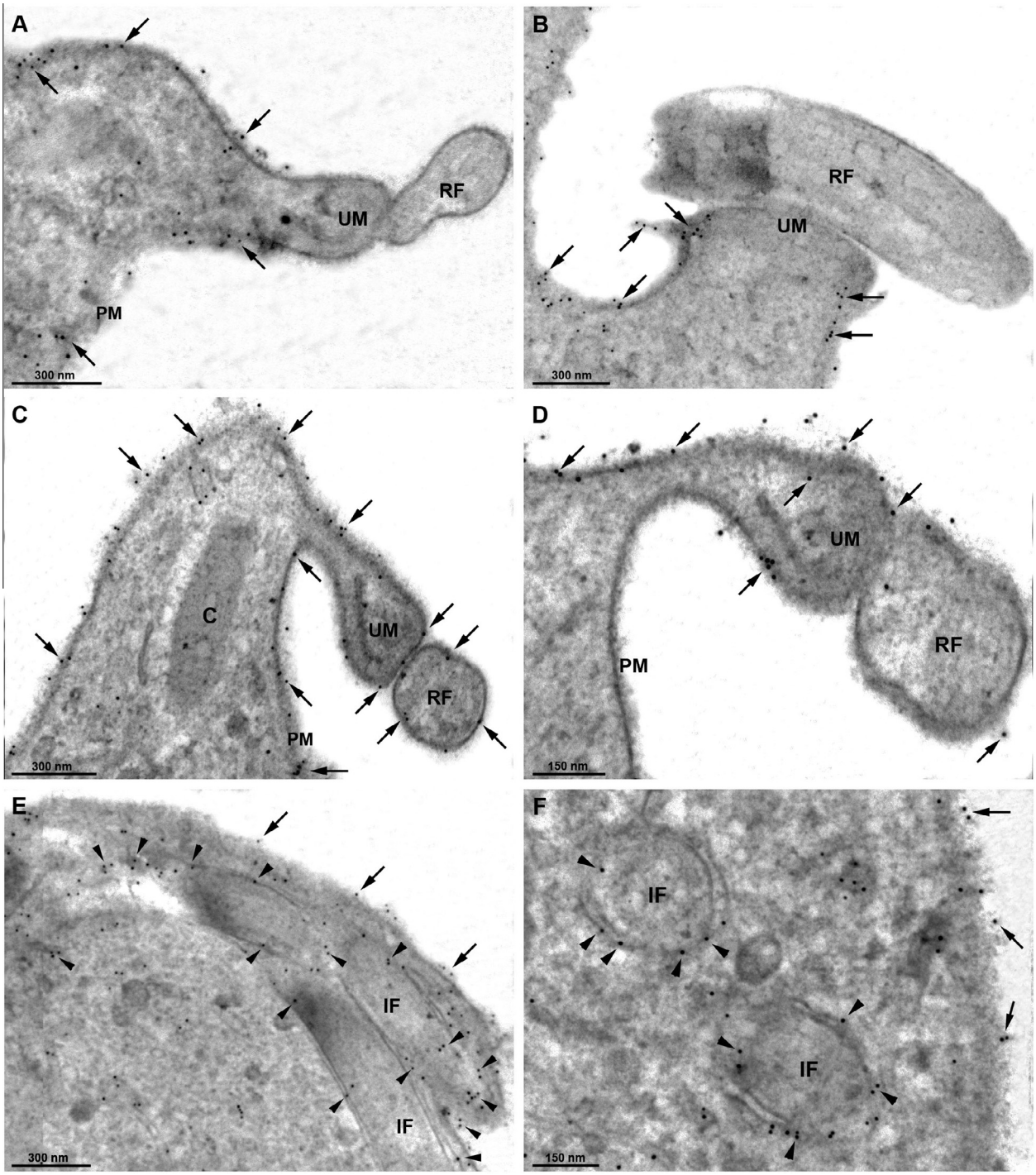

Fig. 9. Immunogold electron microscopy of *T. foetus* using anti-EhPRL antibody. (a,b) Transversal (a) and longitudinal (b) detailed views of the recurrent flagellum (RF) of PS from CC09-1 isolate under standard growth conditions. Gold particles (arrows) are seen on the plasma membrane (PM), but no labelling is observed on the RF and the undulating membrane (UM). (c,d) High magnification of RF of PS from CC09-1 (c) and K (d) strains after 30 min at 4 °C. The UM and the RF surface are labelled (arrows). (e,f) Longitudinal (e) and crossed (f) detailed views of the internalised flagella (IF) of EFF from CC09-1 strain obtained after induction assay. Gold particles are distributed on the PM (arrows), and on the cytoplasmic flagellar canals (arrowheads). C, costa. Bars, a–c, e, 300 nm; d, f, 150 nm.

transformation, immunofluorescence (Fig. 8) and immunogold labelling (Fig. 9) were performed during time-course of EFF induction and reversibility assays. Although PS from CC09-1 isolate exhibited a staining homogeneously distributed on its surface, no labelling was found on the undulating membrane (Figs. 8a,b and 9a,b) and on the plasma membrane of PS from the K strain (Fig. 6a,b). However, after 30 min of EFF induction assay, the undulating membrane and the recurrent flagellum were labelled (Figs. 8c,d and 9c,d) in ~100% of parasites from both strains (n = 3, 300 cells or 100 thin sections). At the beginning of EFF transformation, the parasites (K strain) exhibited a labelling that was distributed in a patchwork pattern on the adjacent cell surface to the recurrent flagellum only (Fig. 8e,f). After 1 h of induction, ~64% of the parasites from K strain undergoing the EFF transformation (n = 3, 300 cells or 100 thin sections) exhibited a surface labelling pattern similar to that found on the parasites from CC09-1 isolate (Fig. 8c,d), whereas ~36% (K strain) showed a staining heterogeneously distributed along the parasites' surface,

Table 2
Effects of anti-EhPRL antibody (dilution 1:200) on *p*-NPP hydrolysis, cytotoxicity and EFF induction and reversibility assays of *T. foetus*.

Condition	K strain		CC09-1 strain	
	PS	EFF	PS	EFF
Rate of p-NPP hydrolysis (nmol p-NP.10^{-7} cells h^{-1}) pH 7.2				
Control	14.00 ± 2.96	58.30 ± 3.49	61.64 ± 3.78	94.10 ± 2.36
After anti-EhPRL pre-treatment	12.26 ± 3.45	10.61 ± 2.31[a]	13.28 ± 4.61[a]	16.82 ± 2.16[a]
Cytotoxicity (1-E/C) after 1.5 h of interaction*				
Control	0.29 ± 0.03	0.55 ± 0.04	0.53 ± 0.02	0.82 ± 0.01
After anti-EhPRL pre-treatment	0.26 ± 0.03	0.22 ± 0.02[a]	0.21 ± 0.03[a]	0.29 ± 0.04[a]
EFF induction and reversibility assays (% parasites)				
Cultures at 25 °C for 4 h	90.64 ± 2.76	9.36 ± 2.76	72.66 ± 3.41	27.34 ± 3.41
Cultures at 25 °C for 4 h after anti-EhPRL pre-treatment	84.99 ± 4.28	15.01 ± 4.28	67.13 ± 3.67	32.87 ± 3.67
Cultures submitted to EFF induction	6.07 ± 1.65[b]	93.93 ± 1.65[b]	3.03 ± 2.7[b]	96.97 ± 2.7[b]
Cultures submitted to EFF induction after anti-EhPRL pre-treatment	48.67 ± 2.67[b,c]	51.33 ± 2.67[b,c]	60.13 ± 4.86[b,c]	39.87 ± 4.86[b,c]
EFF parasites submitted to reversibility assay	88.9 ± 3.91	11.10 ± 3.91	77.64 ± 2.84	22.36 ± 2.84
EFF parasites submitted to reversibility assay after anti-EhPRL pre-treatment	86.43 ± 2.53	13.57 ± 2.53	66.97 ± 2.71	33.03 ± 2.71

Note: The assays were performed as described in Methods section. The values are expressed as the means ± S.D of three independent experiments, each performed in triplicate.
* 1 – (E/C): all measurements of experimental (E) samples were indexed to those of control (C) samples (E/C), which showed no loss of viability, and then subtracted from 1.0.
[a] *p*-value < 0.001 as compared with control.
[b] *p*-value < 0.001 as compared with parasite cultures at 25° for 4 h.
[c] *p*-value < 0.001 as compared with parasite cultures submitted to EFF induction.

presenting a higher fluorescence density on the adjacent region to the recurrent flagellum (Fig. 8g,h). At the end of induction, the surface of ~44% of the EFF from both isolates exhibited a surface labelling heterogeneously distributed in a patchwork pattern (Fig. 8i,j), whereas a homogeneous staining was found on the surface of ~56% (Fig. 8k,l). The EFF also exhibited a labelling on the cytoplasmic flagellar canals (Fig. 9e,f). These results were similar to that found by ultrastructural cytochemistry (Figs. 3 and 4). After the EFF reversibility, the distribution pattern of the anti-EhPRL antibody was similar to that found in PS before EFF induction (not shown). No significant changes were observed in the labelling pattern of permeabilized parasites (not shown).

To investigate whether the protein recognised by anti-EhPRL antibody could be involved in the ecto-phosphatase activities of both forms, intact living PS and EFF were pre-treated with the antibody for 30 min at 25 °C, and the rate of *p*-NPP hydrolysis was measured (Table 2). To rule out the possibility of an antibody-induced capping on the surface antigens, living PS and EFF were immediately fixed after pre-treatment with the primary anti-amoebic antibodies and processed for immunofluorescence. In these assays, the distribution pattern of the anti-EhPRL antibody was similar to that described in Figs. 6 and 8, where the parasites were firstly fixed and, then, incubated with the anti-amoebic antibody (Supplementary Fig. S9). The ecto-phosphatase activity of living PS from K strain was not significantly affected by pre-treatment anti-EhPRL antibody (Table 2). However, the ecto-enzyme activities of pre-treated living PS from CC09-1 isolate and EFF from both isolates were reduced to the same level found in the PS from K strain (Table 2). The anti-EhPRL pre-treatment showed an irreversible effect on these ecto-phosphatase activities (not shown). Similar results were obtained when the enzymatic assays were performed using plasma membrane-enriched fractions (Supplementary Table S2). The anti-EhPTPA and anti-EhPTPB antibodies or pre-immune serum did not affect the enzyme activities of living PS and EFF from both isolates (not shown). BZ3 (3-(3,5-dibromo-4-hydroxy-benzoyl)-2-ethyl-benzofuran-6-sulfonicacid-(4-(thiazol-2-ylsulfamyl)-phenyl)-amide), a specific inhibitor of PTP1b (a classical PTP of mammals and very similar to some PTPs found in Kinetoplastids and *Entamoeba*), did also not affect the ecto-phosphatase activities of both forms (Supplementary Table S1), Taken together, these results indicate that anti-EhPRL antibody could recognise an enzyme responsible for a part of the distinct ecto-phosphatase activities detected between both forms and isolates.

3.4. Effects of the irreversible inhibition of ecto-phosphatase activity on the parasite–host cell interaction and EFF formation

To determine whether the irreversible inhibition of ecto-phosphatase activity was able to affect the interaction of *T. foetus* with host cells, as well the EFF induction and reversion rates, both forms were pre-treated with either anti-EhPRL antibody (Table 2) or 100 μM SO (Supplementary Table S3). Treated and untreated PS and EFF were, then, co-incubated with MDCK cells or submitted to EFF induction and reversibility assays (Table 2; Supplementary Table S3).

After the co-incubation assays, the EFF reversion rate was less than 20% for both isolates. The average number of attached parasites on MDCK cells per microscopic field was similar for PS and EFF from both isolates: ~30 parasites/microscopic field. As expected, after 1.5 h of incubation with parasites under control conditions (no pre-treatment), the cytotoxicity caused by the EFF from both isolates was significantly higher than that of the PS (Table 2; Supplementary Table S3).

After pre-treatment with antibody (Table 2) or SO (Supplementary Table S3), we observed that: (a) the adhesion rate for both forms was not affect (not shown); (b) the cytotoxicity exerted by PS from K strain was not significantly affected, whereas the cytotoxicity exerted by PS from CC09-1 isolate and EFF from both isolates were reduced to the same level found in the PS from K strain; (c) the rates of EFF formation in both isolates were partially inhibited, whereas the rates of EFF reversion was not affect.

The pre-treatment with anti-EhPTPA and anti-EhPTPB antibodies or pre-immune serum had no significant effects on the cytotoxicity and the EFF induction and reversion rates of PS and EFF from both isolates (not shown). BZ3 did also not affect the cytotoxicity and the EFF induction and reversion rates of both isolates (not shown). Because SO inhibits Na^+/K^+-ATPase and others ions transporters, the effects of pre-treatment of ouabain (1.0 mM) and DIDS (1.0 mM) on the parasite–host cell interaction and EFF formation were also evaluated in order to rule out a possible influence of

inhibition of surface ATPases and anion transporters by SO on the experiments. These two compounds did not affect the cytotoxicity and the EFF induction and reversion rates of both isolates (not shown).

4. Discussion

Until now, the most of studies concerning *T. foetus* phosphatases have been performed either with crude parasite lysates (Lockwood et al., 1988; Müller, 1973) or purified enzymes (Gustafson et al., 2005; Thomas et al., 2002), and little is known about their biological functions in living cells. The present study was focused on characterising the ecto-phosphatase activities of intact living PS and EFF *T. foetus* because we were interested in the possible roles of these ecto-enzymes activities on the parasite's transformation and cytotoxicity.

To establish that enzyme activities are due to ecto-enzymes, the following conditions must be met: (a) the enzymes have to act on an extracellular substrate, such as the *p*-NPP; (b) cellular integrity is maintained during enzyme activity; (c) the products are released extracellularly; (d) the enzymes are not released to the extracellular environment; and (e) the enzyme activities can be modified by specific non-penetrating compounds, such as, SO, AM and NaF (Meyer-Fernandes, 2002). In this study, all these criteria were followed and, therefore, our data support the presence of the ecto-phosphatase activities for both *T. foetus* forms. The surface localisation of phosphatase activities was also confirmed by ultrastructural cytochemistry and assays using plasma membrane-enriched fractions. SO, AM and NaF may also inhibit intracellular phosphatases. However, these compounds present a low ability to cross biomembranes because of their negative charges and highly ionised nature (Maccari and Ottana, 2012). In addition, the major biological activity of SO in intact living cells is on the cell surface, because the oxidation–reduction reactions that take place in the cytoplasm decrease its inhibitory effect (Cantley and Aisen, 1979; Dos-Santos et al., 2012).

Lockwood et al. (1988) reported that *T. foetus* releases phosphatases into the culture medium. However, De Jesus et al. (2006) related that this parasite, as opposed to *T. vaginalis* and some trypanosomatids, does not secrete phosphatases to the extracellular medium. The results obtained here are in agreement with those of the De Jesus et al. (2006) because we failed to detect phosphatase activities in the supernatants of either culture or enzyme reaction medium of both forms and isolates. However, our data do not rule out the possibility that some strains of *T. foetus* could be able to secrete phosphatases.

Because our enzymatic assays were performed using intact living parasites or plasma membrane-enriched fractions, the ecto-phosphatase activity detected for *T. foetus* may probably be due to more than one enzyme, as reported for other protists (Andreeva and Kutuzov, 2008; Gomes et al., 2011). In fact, the results of the present study clearly suggest the presence of at least two distinct ecto-phosphatases activities differentially expressed between both *T. foetus* forms and isolates. Similar to our results, previous studies also reported the differential expression of different ecto-phosphatase activities between strains and/or life cycle stages of several parasitic protists, such as *Trypanosoma cruzi* (Dutra et al., 2006; Furuya et al., 1998), *Trypanosoma brucei* (Fernandes et al., 2003), *Trypanosoma rangeli* (Gomes et al., 2006), *Leishmania major* (Aguirre-García et al., 2006) and *Strigomonas culicis* (Catta-Preta et al., 2013), as well in some pathogenic fungal cells (Kneipp et al., 2012; Portela et al., 2010). As observed here during the time-course of EFF transformation, it has been demonstrated that the ecto-phosphatase activities of parasite *Giardia lamblia* also increases during the course of the encystation process (Amazonas et al., 2009).

In most studies concerning ecto-phosphatases, the exact molecular nature of these enzymes has not been determined yet (Andreeva and Kutuzov, 2008). Bakalara et al. (2000) demonstrated that an ecto-phosphatase differentially expressed in the bloodstream form of *T. brucei* may belong to a new enzyme family, lacking homology to other known phosphatases. However, there are evidences that PTPs may be the main enzymes responsible for a large part of ecto-phosphatase activities detected in several pathogenic unicellular microorganisms (Aguirre-García et al., 2003, 2006; Andreeva and Kutuzov, 2008; Furuya et al., 1998; Heneberg, 2012). Similarly, our data also suggest that at least a part of the ecto-phosphatase activities for both *T. foetus* forms exhibit similar characteristics to PTPs.

Little is known concerning PTPs and their biological functions in trichomonads. There are 259 protein sequences of *T. foetus* reported in the GenBank (NCBI), and only one of them is a phosphatase, which is identified as LMW-PTP (Thomas et al., 2002). Because the LMW-PTPs are a group of cytosolic PTPs ubiquitous in eukaryotes and highly conserved from prokaryotes to mammals (Gustafson et al., 2005; Thomas et al., 2002), these enzymes should not be considered as a strong candidate for ecto-phosphatase in *T. foetus*. The lack of a fully sequenced *T. foetus* genome is a factor that complicates the process of understanding and mapping of parasite proteins. Due to this, one strategy is utilises the *T. vaginalis* database to attempt identification by homology.

There are strong evidences suggesting that homologues of classical PTPs very similar to PTP1b from mammals and identified in *E. histolytica*, including the EhPTPA and EhPTPB (Aguirre-García et al., 2003; Herrera-Rodríguez et al., 2006), *Leishmania* spp. (Aguirre-García et al., 2006; Nascimento et al., 2006) and *Trypanosoma* spp. (Gallo et al., 2011; Szoor et al., 2006) may be involved in the ecto-phosphatase activities, the life cycle differentiation and virulence of these parasites. However, in contrast to kinetoplastids and amoeba, classical PTPs homologues are absent in trichomonads (Andreeva and Kutuzov, 2008). This could explain why the anti-EhPTPA and anti-EhPTPB antibodies as well the compound BZ3, a specific inhibitor of classical PTPs, (Gallo et al., 2011; Szoor et al., 2006), did not affect the ecto-phosphatase activities, cytotoxicity and the EFF transformation of *T. foetus*.

PRLs are a subgroup of dual specificity PTPs with an apparent molecular weight of 20- to 25-kDa and a conserved C-terminal prenylation site (Andreeva and Kutuzov, 2008). These enzymes have been implicated in several cellular processes, such as growth, proliferation, cell differentiation, tumorigenesis and metastasis formation (Sun et al., 2007; Zeng et al., 2000). In non-mitotic mammalian cells (Sun et al., 2007; Zeng et al., 2000) and in some parasitic protozoa, such as, *T. cruzi* (Cuevas et al., 2005) and *Plasmodium falciparum* (Pendyala et al., 2008), PRLs have been characterised as an active phosphatase that may be preferentially found on the plasma membrane, early endosome and endoplasmic reticulum. In *E. histolytica*, PRL is a 22-kDa protein that can be localised on the plasma membrane and cytoplasm of trophozoites and their biological functions are unknown (Ramírez-Tapia et al., 2013). Therefore, the molecular weight and the subcellular localisation of *T. foetus* 24-kDa protein recognised by anti-EhPRL antibody support the hypothesis that this protein could be a PRL-like protein.

PRLs have not been detected in *T. vaginalis* (Andreeva and Kutuzov, 2008); however, *in silico* analyses have revealed that the catalytic domain of dual specificity PTPs of the cdc14 subgroup from *T. vaginalis* displays a significant homology with the amino acid sequence of EhPRL (not shown). This finding is expected because it is well known that PRLs are more closely related to PTPs of Cdc14 subgroup (Andreeva and Kutuzov, 2008). PRLs are not ubiquitous in eukaryotes and they may be found in only few

species belonging to the same taxon (Andreeva and Kutuzov, 2008). MALDI mass sequencing of the immunoreactive 24-kDa band was performed in order to get some de novo sequence data; however, at the present moment, no-significant results displaying a better *E*-value and low false positive rates were obtained during protein identification using *T. vaginalis* database. Although *T. foetus* and *T. vaginalis* are close relatives, they may have many differences with respect to nucleotide sequences, suggesting that their proteins could not have sufficient homology to make this a useful strategy (Greenwell et al., 2008). Our current investigations focus on sequencing of full *T. foetus* genome to precisely identify the PRL-like protein and the presence of other PTPs in the parasite.

Based on our data concerning the immunodetection and inhibition assays using anti-EhPRL antibody, we propose that the expression or up-regulation of the 24-kDa protein on the parasite's surface could be responsible by a part of the ecto-phosphatase activities differentially expressed between PS and EFF, as well between strains. However, our data does not exclude that other ecto-phosphatases may be involved in these enzyme activities. The inhibition induced by anti-EhPRL could be due that the antibodies are recognising 3D epitopes within the structurally conserved PTP domain that are critical for the enzymatic activity, or that the antibody binding destabilizes the PRL-like protein in such a way that the ecto-enzyme is not able to recognise it substrate. Further studies are needed to clarify this issue.

Immunoelectron microscopy suggests that *T. foetus* PRL-like protein could be translocated to the plasma membrane via exocytosis. In intraerythrocytic stages of *P. falciparum*, the PRL is associates with endoplasmic reticulum and a subcompartment of the food vacuole; however, in maturing merozoites, this enzyme may be translocated to the cell surface (Pendyala et al., 2008). Similarly, in promastigotes of *Leishmania mexicana*, the overexpression of an ecto-phosphatase located in the endosomal compartment leads to its abundant exposure on the parasite surface (Wiese et al., 1996).

The biological mechanisms that regulate the transformation of the polarised PS form into the EFF have not been elucidated yet. Here, it was shown that EFF induction, but not its reversion, was partially blocked when a part of ecto-phosphatase activities of PS parasites was irreversibly inhibited. Therefore, our results suggest that the ecto-phosphatase activities of *T. foetus* could play a physiological role during the EFF transformation. Similarly, there are strong evidences suggesting that ecto-phosphatases activities could regulate morphological transitions in some pathogenic fungi (Alviano et al., 2003; Kneipp et al., 2012) and protozoa, such as, *G. lamblia* (Amazonas et al., 2009), *Trypanosoma* spp. (Bakalara et al., 2000; Furuya et al., 1998; Gomes et al., 2006) and *Leishmania* spp. (Aguirre-García et al., 2006; Nascimento et al., 2006). Based on our ultrastructural data, it is tempting to speculate that the ecto-phosphatase activities could signal the process of flagella internalisation during EFF formation. However, further studies are needed to determine the exact role of the *T. foetus* ecto-phosphatase activities during the process of transformation.

The detection of cell surface-localised phosphatase activity is particularly interesting due to its possible role in the process of host–parasite interactions (Gomes et al., 2011). In the present study, the irreversible inhibition of a part of the ecto-phosphatase activities partially reduced the cytotoxic effects exerted by both *T. foetus* forms, indicating that the ecto-phosphatase activities could provide an additional mechanism for cytotoxicity of *T. foetus*. Similarly, some reports have demonstrated that the cytotoxicity of *E. histolytica* (Aguirre-García et al., 2003) and *Leishmania amazonensis* (Martiny et al., 1999) on the host cells was abolished when the parasites were pre-treated with PTP inhibitors. Moreover, Aguirre-García et al. (2003) demonstrated that a membrane-bound PTP from *E. histolytica* is able to induce cytotoxic effects by the disruption of the host cell actin microfilaments. Further studies are needed to determine the exact role of *T. foetus* ecto-phosphatase activities during its pathogenic process.

Some reports also demonstrated that the irreversible inhibition of the ecto-phosphatase activities of some pathogenic Kinetoplastids (Catta-Preta et al., 2013; Dos-Santos et al., 2012) and fungi (Kneipp et al., 2012; Portela et al., 2010) provokes a reduction in their ability to attach to host epithelial cells. In contrast, the results presented here suggest that the ecto-phosphatase activities of both *T. foetus* forms could not be involved in the process of parasite adhesion to host cells.

Several studies have reported that ecto-phosphatase activities may represent an important virulence marker for some parasitic fungi and protists (De Jesus et al., 2006; Dutra et al., 2006; Gomes et al., 2011; Heneberg, 2012). In agreement, here, a positive correlation was observed between ecto-phosphatase activity, surface expression of PRL-like protein and the cytotoxicity exerted by both *T. foetus* forms to epithelial cells. Therefore, our data support the hypothesis that the rate of ecto-phosphatase activity and the surface expression of PRL-like protein could represent virulence markers for *T. foetus*.

In conclusion, to our knowledge, the present study demonstrates for the first time that the ecto-phosphatase activities on intact living *T. foetus* may differ in expression, biochemical properties and ultrastructural localisation between PS and EFF, as well, between low- and high-cytotoxic strains. Furthermore, this study brings to light additional evidences concerning the possible participation of the ecto-phosphatase activities during the EFF transformation and cytotoxicity of *T. foetus*. The knowledge of how ecto-phosphatases potentially contribute to EFF formation and pathogenesis of *T. foetus* may be useful to reveal new mechanisms involved in the infectious process during trichomonosis and provide a promising target for chemotherapy.

Acknowledgments

This work was supported by Conselho Nacional de Desenvolvimento Científico e Tecnológico (CNPq), Fundação Carlos Chagas Filho de Amparo à Pesquisa do Estado do Rio de Janeiro (FAPERJ), Programa de Núcleos de Excelência (PRONEX), Coordenação de Aperfeiçoamento de Pessoal de Nível Superior (CAPES) and Associação Universitária Santa Úrsula (AUSU).

Appendix A. Supplementary data

Supplementary data associated with this article can be found, in the online version, at http://dx.doi.org/10.1016/j.exppara.2014.04.007.

References

Aguirre-García, M.M., Anaya-Ruiz, M., Talamás-Rohana, P., 2003. Membrane-bound acid phosphatase (MAP) from *Entamoeba histolytica* has phosphotyrosine phosphatase activity and disrupts the actin cytoskeleton of host cells. Parasitology 126, 195–202.

Aguirre-García, M.M., Escalona-Montaño, A.R., Bakalara, N., Pérez-Torres, A., Gutiérrez-Kobeh, L., Becker, I., 2006. *Leishmania major*: detection of membrane-bound protein tyrosine phosphatase. Parasitology 132, 641–649.

Alviano, D.S., Kneipp, L.F., Lopes, A.H., Travassos, L.R., Meyer-Fernandes, J.R., Rodrigues, M.L., Alviano, C.S., 2003. Differentiation of *Fonsecaea pedrosoi* mycelial forms into sclerotic cells is induced by platelet-activating factor. Res. Microbiol. 154, 689–695.

Amazonas, J.N., Cosentino-Gomes, D., Werneck-Lacerda, A., Pinheiro, A.A., Lanfredi-Rangel, A., De Souza, W., Meyer-Fernandes, J.R., 2009. *Giardia lamblia*: characterization of ecto-phosphatase activities. Exp. Parasitol. 121, 15–21.

Andreeva, A.V., Kutuzov, M.A., 2008. Protozoan protein tyrosine phosphatases. Int. J. Parasitol. 38, 1279–1295.

Bahta, M., Burke, T.R., 2012. *Yersinia pestis* and approaches to targeting its outer protein H protein-tyrosine phosphatase (YopH). Curr. Med. Chem. 19, 5726–5734.

Bakalara, N., Santarelli, X., Davis, C., Baltz, T., 2000. Purification, cloning, and characterization of an acidic ectoprotein phosphatase differentially expressed in the infectious bloodstream form of *Trypanosoma brucei*. J. Biol. Chem. 275, 8863–8871.

BonDurant, R.H., 2005. Venereal diseases of cattle: natural history, diagnosis, and the role of vaccines in their control. Vet. Clin. North Am. Food Anim. Pract. 21, 383–408.

Cantley Jr., L.C., Aisen, P., 1979. The fate of cytoplasmic vanadium. Implications on (NA, K)-ATPase inhibition. J. Biol. Chem. 254, 1781–1784.

Catta-Preta, C.M., Nascimento, M.T., Garcia, M.C., Saraiva, E.M., Motta, M.C., Meyer-Fernandes, J.R., 2013. The presence of a symbiotic bacterium in *Strigomonas culicis* is related to differential ecto-phosphatase activity and influences the mosquito–protozoa interaction. Int. J. Parasitol. 43, 571–577.

Cosentino-Gomes, D., Meyer-Fernandes, J.R., 2011. Ecto-phosphatases in protozoan parasites: possible roles in nutrition, growth and ROS sensing. J. Bioenerg. Biomembr. 43, 89–92.

Cuevas, I.C., Rohloff, P., Sánchez, D.O., Docampo, R., 2005. Characterization of farnesylated protein tyrosine phosphatase TcPRL-1 from *Trypanosoma cruzi*. Eukaryot. Cell. 4, 1550–1561.

De Jesus, J.B., Podlyska, T.M., Hampshire, A., Lopes, C.S., Vannier-Santos, M.A., Meyer-Fernandes, J.R., 2002. Characterization of an ecto-phosphatase activity in the human parasite *Trichomonas vaginalis*. Parasitol. Res. 11, 991–997.

De Jesus, J.B., Ferreira, M.A., Cuervo, P., Britto, C., e Silva-Filho, F.C., Meyer-Fernandes, J.R., 2006. Iron modulates ecto-phosphohydrolase activities in pathogenic trichomonads. Parasitol. Int. 55, 285–290.

Diamond, L.S., 1957. The establishment of various trichomonads of animals and man in axenic cultures. J. Parasitol. 43, 488–490.

Díaz, J.A., Monteiro-Leal, L.H., de Souza, W., 1996. Isolation and biochemical characterization of the plasma membrane of *Tritrichomonas foetus*. BioCell 20, 21–31.

Dos-Santos, A.L., Dick, C.F., Alves-Bezerra, M., Silveira, T.S., Paes, L.S., Gondim, K.C., Meyer-Fernandes, J.R., 2012. Interaction between *Trypanosoma rangeli* and the *Rhodnius prolixus* salivary gland depends on the phosphotyrosine ecto-phosphatase activity of the parasite. Int. J. Parasitol. 42, 819–827.

Dutra, P.M., Couto, L.C., Lopes, A.H., Meyer-Fernandes, J.R., 2006. Characterization of ecto-phosphatase activities of *Trypanosoma cruzi*: a comparative study between Colombiana and Y strains. Acta Trop. 100, 88–95.

Fernandes, E.C., Mauro Granjeiro, J., Mikio Taga, E., Meyer-Fernandes, J.R., Aoyama, H., 2003. Phosphatase activity characterization on the surface of intact bloodstream forms of *Trypanosoma brucei*. FEMS Microbiol Lett. 220, 197–206.

Fiske, C.H., Subbarow, Y., 1925. The colorimetric determination of phosphorus. J. Biol. Chem. 66, 375–400.

Furuya, T., Zhong, L., Meyer-Fernandes, J.R., Lu, H.G., Moreno, S.N.J., Docampo, R., 1998. Ecto-protein tyrosine phosphatase activity in *Trypanosoma cruzi* infective stages. Mol. Biochem. Parasitol. 92, 339–348.

Gallo, G., Ramos, T.C., Tavares, F., Rocha, A.A., Machi, E., Schenkman, S., Bahia, D., Pesquero, J.B., Würtele, M., 2011. Biochemical characterization of a protein tyrosine phosphatase from *Trypanosoma cruzi* involved in metacyclogenesis and cell invasion. Biochem. Biophys. Res. Commun. 408, 427–431.

Gomes, S.A., Fonseca de Souza, A.L., Silva, B.A., Kiffer-Moreira, T., Santos-Mallet, J.R., Santos, A.L., Meyer-Fernandes, J.R., 2006. *Trypanosoma rangeli*: differential expression of cell surface polypeptides and ecto-phosphatase activity in short and long epimastigote forms. Exp. Parasitol. 112, 253–262.

Gomes, M.T., Lopes, A.H., Meyer-Fernandes, J.R., 2011. Possible roles of ectophosphatases in host–parasite interactions. J. Parasitol. Res.. http://dx.doi.org/10.1155/2011/479146.

Greenwell, P., Younes, M., Rughooputh, S., 2008. Purification and analysis of DNases of *Tritrichomonas foetus*: evidence that these enzymes are glycoproteins. Int. J. Parasitol. 38, 749–756.

Gustafson, C.L., Stauffacher, C.V., Hallenga, K., Van Etten, R.L., 2005. Solution structure of the low-molecular-weight protein tyrosine phosphatase from *Tritrichomonas foetus* reveals a flexible phosphate binding loop. Protein Sci. 14, 2515–2525.

Heneberg, P., 2012. Finding the smoking gun: protein tyrosine phosphatases as tools and targets of unicellular microorganisms and viruses. Curr. Med. Chem. 19, 1530–1566.

Herrera-Rodríguez, S.E., Baylón-Pacheco, L., Talamás-Rohana, P., Rosales-Encina, J.L., 2006. Cloning and partial characterization of *Entamoeba histolytica* PTPases. Biochem. Biophys. Res. Commun. 342, 1014–1021.

Kneipp, L.F., Magalhães, A.S., Abi-Chacra, E.A., Souza, L.O., Alviano, C.S., Santos, A.L., Meyer-Fernandes, J.R., 2012. Surface phosphatase in *Rhinocladiella aquaspersa*: biochemical properties and its involvement with adhesion. Med. Mycol. 50, 570–578.

Lockwood, B.C., North, M.J., Coombs, G.H., 1988. The release of hydrolases from *Trichomonas vaginalis* and *Tritrichomonas foetus*. Mol. Biochem. Parasitol. 30, 135–142.

Lowry, O.H., Rosebrough, N.J., Farr, A.L., Randall, R.J., 1951. Protein measurement with the Folin phenol reagent. J. Biol. Chem. 193, 265–275.

Maccari, R., Ottana, R., 2012. Low molecular weight phosphotyrosine protein phosphatases as emerging targets for the design of novel therapeutic agents. J. Med. Chem. 55, 2–22.

Madeiro da Costa, R.F., Benchimol, M., 2004. The effect of drugs on cell structure of *Tritrichomonas foetus*. Parasitol. Res. 92, 159–170.

Manning, K., 2010. Update on the diagnosis and management of *Tritrichomonas foetus* infections in cats. Top. Companion. Anim. Med. 25, 145–148.

Mardones, F.O., Perez, A.M., Martínez, A., Carpenter, T.E., 2008. Risk factors associated with *Tritrichomonas foetus* infection in beef herds in the Province of Buenos Aires. Argentina. Vet. Parasitol. 153, 231–237.

Martiny, A., Meyer-Fernandes, J.R., de Souza, W., Vannier-Santos, M.A., 1999. Altered tyrosine phosphorylation of ERK1 MAP kinase and other macrophage molecules caused by *Leishmania* amastigotes. Mol. Biochem. Parasitol. 102, 1–12.

Meyer-Fernandes, J.R., 2002. Ecto-ATPases in protozoa parasites: looking for a function. Parasitol. Int. 51, 299–303.

Müller, M., 1973. Biochemical cytology of trichomonad flagellates. I. Subcellular localization of hydrolases, dehydrogenases, and catalase in *Tritrichomonas foetus*. J. Cell Biol. 57, 453–474.

Nascimento, M., Zhang, W.W., Ghosh, A., Houston, D.R., Berghuis, A.M., Olivier, M., Matlashewski, G., 2006. Identification and characterization of a protein-tyrosine phosphatase in *Leishmania*: involvement in virulence. J. Biol. Chem. 281, 36257–36268.

Pendyala, P.R., Ayong, L., Eatrides, J., Schreiber, M., Pham, C., Chakrabarti, R., Fidock, D.A., Allen, C.M., Chakrabarti, D., 2008. Characterization of a PRL protein tyrosine phosphatase from *Plasmodium falciparum*. Mol. Biochem. Parasitol. 158, 1–10.

Pereira-Neves, A., Benchimol, M., 2009. *Tritrichomonas foetus*: budding from multinucleated pseudocysts. Protist 160, 536–551.

Pereira-Neves, A., Campero, C.M., Martínez, A., Benchimol, M., 2011. Identification of *Tritrichomonas foetus* pseudocysts in fresh preputial secretion samples from bulls. Vet. Parasitol. 175, 1–8.

Pereira-Neves, A., Nascimento, L.F., Benchimol, M., 2012. Cytotoxic effects exerted by *Tritrichomonas foetus* pseudocysts. Protist 163, 529–543.

Portela, M.B., Kneipp, L.F., Ribeiro de Souza, I.P., Holandino, C., Alviano, C.S., Meyer-Fernandes, J.R., de Araújo Soares, R.M., 2010. Ectophosphatase activity in *Candida albicans* influences fungal adhesion: study between HIV-positive and HIV-negative isolates. Oral Dis. 16, 431–437.

Ramírez-Tapia, A.L., Pérez-Saldaña, J.A., López, F.S., Baylón-Pacheco, L., Gordillo, P.E., Guaderrama-Díaz, M., Rosales-Encina, J.L., 2013. Phosphatase protein tyrosine of *Entamoeba histolytica*. In: Butanda, A., Guevara-Flores, A., Guevara-Fonseca, J., Matuz-Mares, D., Rendón, E., Vázquez-Meza, H. (Eds.), Mensaje Bioquímico, vol. XXXVII. Depto. de Bioquímica, Facultad de Medicina, Universidad Nacional Autónoma de México. C. Universitaria, México, DF, pp. 241–260.

Sun, J.P., Luo, Y., Yu, X., Wang, W.Q., Zhou, B., Liang, F., Zhang, Z.Y., 2007. Phosphatase activity, trimerization, and the C-terminal polybasic region are all required for PRL1-mediated cell growth and migration. J. Biol. Chem. 282, 29043–29051.

Szoor, B., Wilson, J., McElhinney, H., Tabernero, L., Matthews, K.R., 2006. Protein tyrosine phosphatase TbPTP1: a molecular switch controlling life cycle differentiation in trypanosomes. J. Cell Biol. 175, 293–303.

Thomas, C.L., McKinnon, E., Granger, B.L., Harms, E., Van Etten, R.L., 2002. Kinetic and spectroscopic studies of *Tritrichomonas foetus* low-molecular weight phosphotyrosyl phosphatase. Hydrogen bond networks and electrostatic effects. Biochemistry 41, 15601–15609.

Tonks, N.K., 2013. Protein tyrosine phosphatases: from housekeeping enzymes to master regulators of signal transduction. FEBS J. 280, 346–378.

Wiese, M., Berger, O., Stierhof, Y.D., Wolfram, M., Fuchs, M., Overath, P., 1996. Gene cloning and cellular localization of a membrane-bound acid phosphatase of *Leishmania mexicana*. Mol. Biochem. Parasitol. 82, 153–165.

Zeng, Q., Si, X., Horstmann, H., Xu, Y., Hong, W., Pallen, C.J., 2000. Prenylation-dependent association of protein-tyrosine phosphatases PRL-1, -2, and -3 with the plasma membrane and the early endosome. J. Biol. Chem. 275, 21444–21452.